

Satellite Digital Audio Radio Service Front-End

By:
Keven Lockwood

Advisor:
Dr. Prasad Shastry

Senior Capstone Project Final Report



Department of Electrical and Computer Engineering

Spring 2011

Abstract

Since its inception in 2002, satellite radio has provided consumers with reliable radio entertainment with subscription access to over 100 channels via a store-bought receiver. It accomplished the goal of uninterrupted reception of a single radio station while travelling across the country. One of the most important components of the receiver system is the active antenna, known as the front-end. Originating from a base station on the ground, radio signals are transmitted to orbiting satellites in space, which are then broadcasted and received by the front-end.

The purpose of this project is to design the active antenna for use with a Sirius ® radio system. An active antenna consists of a passive antenna and a paired low-noise amplifier. The antenna type used in the project consists of a perturbed, rectangular, metallic patch and a proximity-coupled feed-line. The patch and feed-line are separated by a dielectric substrate. Important considerations in antenna design are frequency of operation, gain, and polarization.

The low-noise amplifier (LNA) that is integrated with the patch antenna increases the relatively weak signal received by the antenna while introducing a minimum amount of noise for adequate signal quality. Important considerations in LNA design are frequency of operation, gain, and noise figure.

This report contains a functional description, summary of literature and past work, design of a circularly polarized patch antenna with proximity-coupled feed, simulations, fabrication, testing, and future improvements.

Acknowledgements

I would like to thank Dr. Prasad Shastry for his continued support and advice throughout the project.

I would like to thank Dr. Brian Huggins for his swift assistance in part purchasing and moral support.

I would like to thank James O'Donnell for his support in the RF laboratory and throughout the fabrication process.

I would like to thank Sundar Vinod for his support in the RF lab and advice on use of Advanced Design System and Momentum.

I would like to thank David miller for his assistance in the final steps of antenna fabrication.

Table of Contents

Abstract.....	i
Acknowledgements.....	ii
Chapter 1 Introduction.....	1
Chapter 2 Functional Description.....	2
2.1 Introduction.....	2
2.2 SDARS Functions.....	2
2.3 Concluding Remarks.....	4
Chapter 3 Literature Review.....	4
3.1 Introduction.....	4
3.2 Project Specifications and Discussion.....	5
A Antenna VSWR, Angle of Reception, and Bandwidth.....	5
B Antenna Polarization.....	6
C Low-Noise Amplifier.....	8
3.3 Earlier Work Summary.....	9
3.4 Concluding Remarks.....	10
Chapter 4 Microstrip Patch Antenna Design and Simulations.....	11
4.1 Introduction.....	11
4.2 Linearly Polarized Antenna Design and Simulations.....	12
4.3 Circularly Polarized Antenna Design and Simulations.....	17
4.4 Circularly Polarized Antenna Feed Line Matching Network.....	21
4.5 Concluding Remarks.....	24
Chapter 5 Circularly Polarized Antenna Fabrication and Measurements.....	24
5.1 Introduction.....	24
5.2 Antenna Fabrication.....	24
5.3 Antenna Measurements.....	25
5.4 Concluding Remarks.....	27
Chapter 6 Low-Noise Amplifier Subsystem.....	28
6.1 Introduction.....	28
6.2 LNA Subsystem.....	28
6.3 LNA Measurements.....	29
6.4 Concluding Remarks.....	30
Chapter 7 SDARS Front-End Testing and Post-Fabrication Simulations.....	30
7.1 Introduction.....	30
7.2 SDARS Front-End Test.....	31
7.3 Post-Fabrication Simulations.....	33
7.4 Concluding Remarks.....	35
Chapter 8 Conclusion and Future Suggestions.....	35
References	
Appendix A: Simulated Axial Ratio Measurements	
Appendix B: Printing Designs in ADS for Technicraft Corporation	
Appendix C: Perturbed Patch Antenna and Final Matching Network	
Appendix D: Measurement of Axial Ratio in Anechoic chamber	
Appendix E: Data Sheets of Amplifiers	

Chapter 1

Introduction

SDARS stands for the Satellite Digital Audio Radio Service. Since its beginnings in 2002, the Federal Communications Commission has allocated a portion of the frequency spectrum, 2.32 to 2.345 GHz, to two companies who implemented satellite radio: Sirius ® and XM. Sirius ® would operate in the band from 2.32 to 2.3325 GHz and XM between 2.3325 to 2.345 GHz. These two companies provide high-definition subscription radio with 200 channels between them over a much wider reception range than the existing FM radio towers. Because the transmissions arrive from space, use of three satellites is adequate to provide continuous reception over the entirety of the United States. Today, Sirius ® and XM have merged to one company, but still keep their product lines relatively separate.

In order to extract the electromagnetic signals from these satellites, an antenna is used as a medium to transition the signals onto a wire connected to some type of radio receiver. This project focuses on the passive antenna design and immediate amplification of received signals through an integrated low-noise amplifier, which is called the front-end or active antenna. The signals going into the receiver must be between a certain power level range while introducing as little noise power as possible for adequate signal-to-noise ratio.

The purpose of this project is to design and fabricate the front-end to be able to receive Sirius ® radio signals from orbiting satellites in the frequency band from 2.32 to 2.3325 GHz. The amplified output will then be fed directly to a commercially available receiver manufactured by Sirius ®, which handles the remaining signal conditioning so entertainment audio can be heard when connecting a pair of speakers to the device. This project is purely educational in nature; no new antenna designs will be introduced or have publishable information. It is only a means to increase one's knowledge of radio frequency circuits.

The basis for the antenna design originates from [1]. A microstrip antenna with a proximity-coupled feedline is used. By offsetting the feedline from the center of the radiating patch, the antenna is able to receive circularly polarized transmissions. In further reading of this report, a design change was made to increase this ability further. Perturbations were introduced in the patch geometry and the feedline moved back to the center, as described in [2] and [3].

By the end of the spring semester 2011, one proximity-coupled antenna with perturbations in the patch structure was fabricated and tested for return loss, gain, and axial ratio. Due to fabrication imperfections, the ideal operating frequency range of the antenna is greater than the desired band and the axial ratio degraded significantly, yet the antenna will still receive Sirius ® transmissions. In the interest of time, the amplification circuitry was kept modular. An appropriate amplifier surface-mount package was researched and the evaluation board used as a temporary means to demonstrate front-end functionality.

Chapter 2 Functional Description

2.1 Introduction

This section describes how SDARS transmits its signals and where the project focus fits into the overall system.

2.2 SDARS Functions

In fig 2.1, a base station operated by the Sirius ® radio company transmits signals to orbiting satellites. These satellites repeat the signal by broadcasting it over an extremely wide area as indicated by one satellite. The broadcasted signals can be received by consumer antennas via a direct line of site, or through terrestrial repeaters if the signal is blocked. Terrestrial repeaters are located on the ground in areas where the direct line of sight is obstructed, such as in

tunnels or in urban areas with tall buildings. This project is concerned with reception of the direct transmissions only.

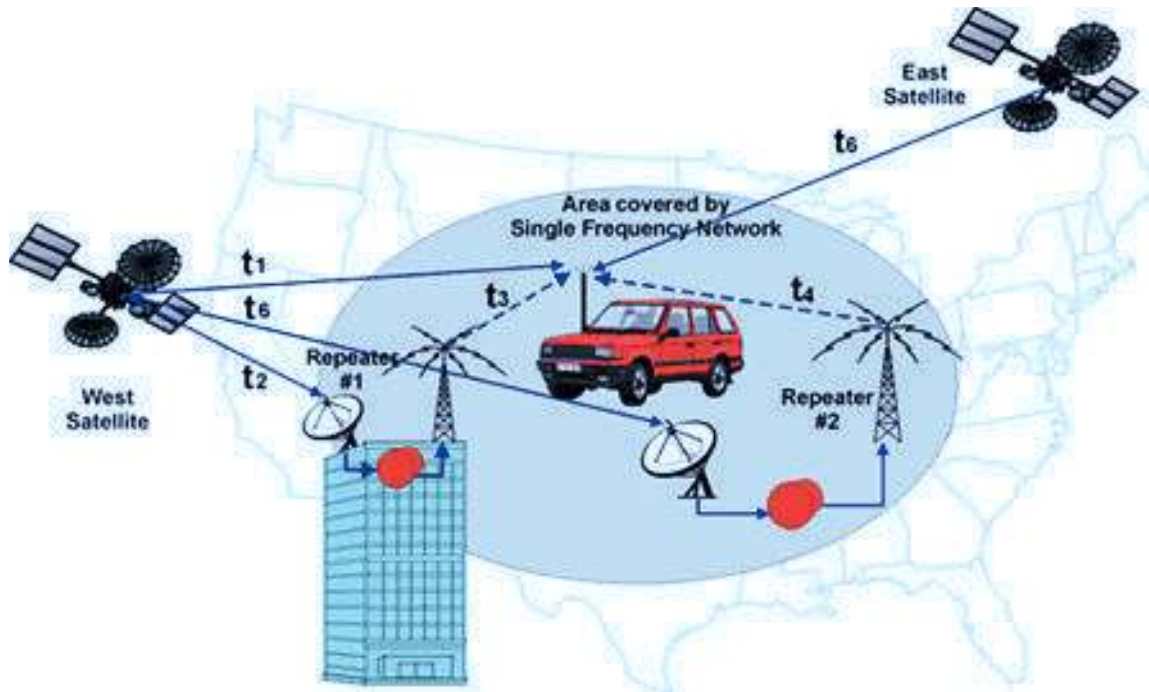


Fig. 2.1 Visual diagram of how SDARS functions
(<http://cegt201.bradley.edu/projects/proj2001/sdarsprj/funcdesc.html>)

Fig. 2.2 shows where the project fits into the overall function of a radio system. Signals from a satellite arrive at a passive antenna, generating AC currents on the antenna structure. These currents translate into electromagnetic waves on the antenna's feedline, which is connected to the low-noise amplifier. Because the signal is very low in power (-105 to -95 dBm) when it reaches the receiving antenna [4], Proper amplification of the signal is necessary for the receiver to perform any further processing. The amplification circuitry must introduce as little noise power as possible so that adequate signal-to-noise ratio is produced at the input to the receiver. To reduce the amount of noise generated by the active antenna, the amplification circuit must be placed as close to the output of the antenna as possible. It is well known that the overall

noise power produced is contributed primarily by the passive antenna and first stage of amplification (if multiple stages are used). Due to this fact, the amplifier used in the first stage should have high gain and a low noise figure (a measure of signal degradation in a system).

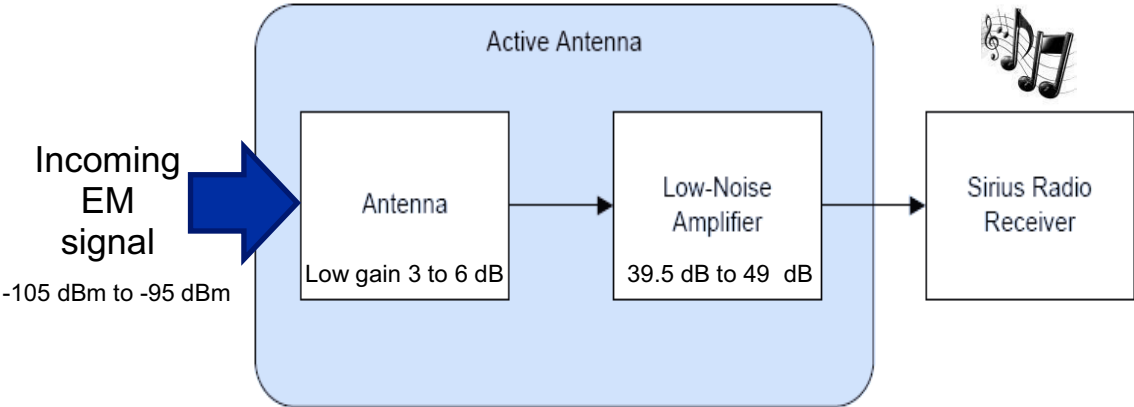


Fig. 2.2 Overall Project Functional Block Diagram

2.3 Concluding Remarks

It is noteworthy that the active antenna does not perform signal processing other than simple amplification. All further steps of the process to create audio are handled by the Sirius[®] radio receiver, and so its functional description is outside the scope of this project.

Chapter 3 Literature Review

3.1 Introduction

This chapter describes the different sources consulted, leading to the fabrication of the proximity-coupled patch antenna designed in this project.

3.2 Project Specifications and Discussion

A. Antenna VSWR, Angle of reception, and Gain

The specifications for the passive antenna are given in Table 3.1. The voltage standing wave ratio (VSWR) determines the operating frequency range of the antenna, conforming to the band in which Sirius ® radio transmits. The VSWR is directly related to the reflection coefficient, S11 (the ratio of a reflected wave amplitude to an incident wave amplitude introduced at the antenna port). If there is no reflection, S11 is 0 and hence VSWR = 1, the ideal case. We can define the band of operation of an antenna by the two extreme frequencies that give a VSWR of 2. The antenna is not tuned to the target band if a VSWR greater than 2 is measured inside this range. S11 and VSWR are measured using a network analyzer.

Table 3.1
Passive Antenna Specifications [4]

Parameter	Minimum	Typical	Maximum
VSWR	1		2
Angle of Reception	90°		130°
Passive gain		3 dBic	
Axial Ratio (LHCP)	0 dB		3 dB

The angle of reception describes how much the antenna may be angled from the transmission normal to the patch surface and still receives adequate signal power. We can define the angular width of the main lobe of a plot picturing the antenna radiation pattern as the beamwidth (see fig. 3.1). The angle at which the antenna receives half power on each side of the main lobe constitutes the 3-dB beamwidth. We may consider these to define the maximum angle of reception. This can be measured by generating a rectangular beam pattern plot using the anechoic chamber test bench.

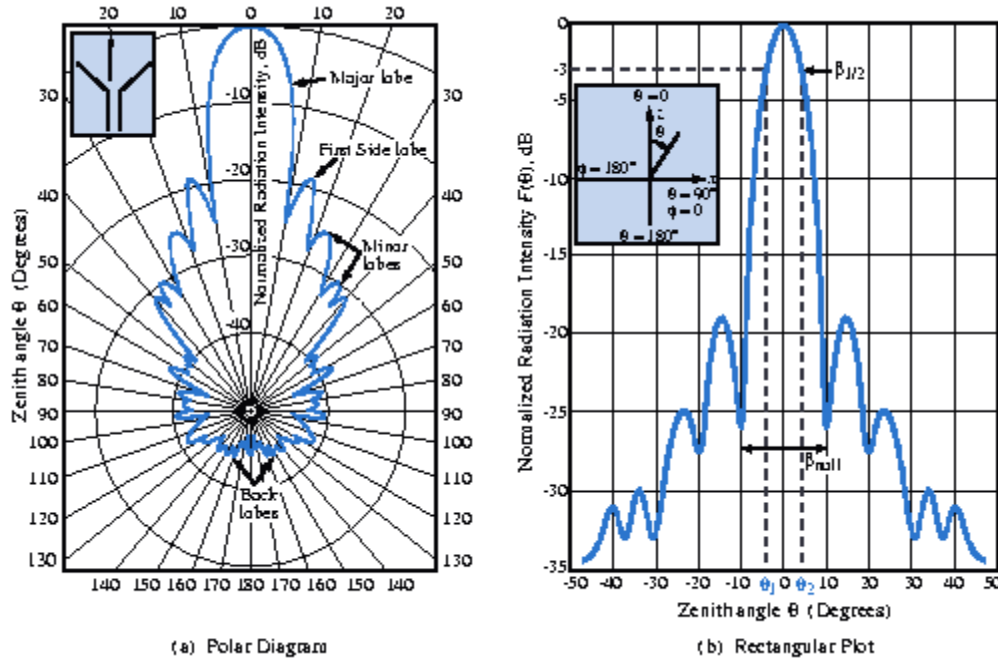


Fig. 3.1 An example of a normalized polar and rectangular plot showing an antenna radiation pattern [5]

The passive antenna gain is a measure of the antenna’s ability to focus EM energy coming from a particular direction with respect to an isotropic radiator. Energy incident on the antenna is focused, so the signal power at the antenna port is greater than the incident power. The ratio of these is the antenna gain. This is measured using the anechoic chamber and the well-known Friis transmission formula given in (3.1). The gains G_t and G_r are equal for identical antennas used for transmitting and receiving. There is little control over this parameter when optimizing designs for other parameters, so the amplification circuitry can compensate. Patch antennas have typically exhibited around 3dB gain.

$$P_r = \frac{P_t G_t G_r \lambda^2}{(4\pi R)^2} \quad (3.1)$$

B. Antenna Polarization

The axial ratio measures the antenna’s ability to receive a circularly polarized EM transmission. According to [5], “Wave polarization describes the shape and locus of the tip of the

E-field vector (in the plane orthogonal to the direction of propagation) at a given point in space as a function of time.” A perfect circularly polarized (CP) wave E-field vector will rotate in a circle with equal magnitude. It is the ideal case to an elliptically polarized wave, as shown in fig. 3.2. The orthogonal component magnitudes of the wave are represented by the major and minor axis. The ratio of the larger to the smaller gives the Axial Ratio, which is 1 for the perfect case. Using the Anechoic chamber and a linearly polarized antenna as the transmitter, the received power can be obtained with the antenna upright and then turned 90° . Using these measurements, an antenna may be considered CP if the axial ratio is less than 3 dB.

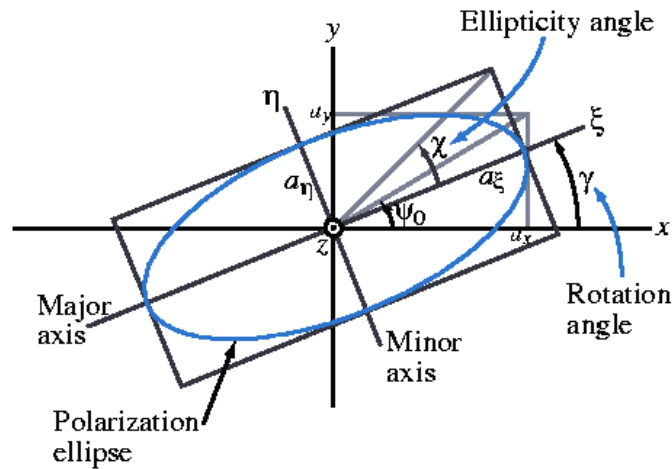


Fig. 3.2 An elliptically polarized wave propagating out of the page [5]

While the axial ratio describes how circular polarized an antenna is, it does not define whether it can receive left-hand circularly polarized (LHCP) or right-hand circularly polarized (RHCP) waves. With the former, the electric field vector rotates in the clockwise direction as in fig. 3.2. RHCP waves rotate counterclockwise. The antenna designed for this project must be LHCP. To test for this, transmitting LHCP and RHCP antennas are used in the anechoic chamber. Each transmitter radiates a wave with their particular polarization and the signal is received by the project antenna. There should be significant attenuation of the received signal if

the two transmitting and receiving antenna polarizations are mismatched and good reception when they are matched.

C. Low-Noise Amplifier

The specifications for the low-noise amplifier (LNA) subsystem are shown in table 3.2. It is connected directly to the passive antenna output.

Table 3.2
LNA subsystem specifications [4]

Parameter	Minimum	Typical	Maximum
Gain	39.5 dB		49 dB
Noise Figure		0.7 dB	0.9 dB
Operating Frequency	2.32 GHz		2.3325 GHz

The gain of the LNA system increases the signal power enough so the receiver can process it, since the incoming signal has such low power. Two amplifiers were needed to meet this specification.

The noise figure measures the amount of signal to noise ratio degradation introduced by the LNA subsystem. Two cascaded amplifiers were chosen through research that provide high gain and low noise figure. In (3.2), the primary contributor of noise in a system is the first stage of amplification, as long as amplification by the first stage (G_1) is high. Components afterwards contribute very little to the overall noise factor. The noise figure is the noise factor measurement in decibels.

Testing of the LNA system for the noise figure involves connecting a noise source at the input of the LNA and measuring the output noise power while the source is unpowered (cold) and powered (hot). Using the specification of the excess noise ratio (ENR) of the source and the

Y factor, overall noise factor can be calculated. This is a very good approximation of the noise generated by the single stage (see fig. 3.3).

$$F_t = F_1 + \frac{F_2 - 1}{G_1} + \frac{F_3 - 1}{G_1 G_2} + \dots \quad (3.2)$$

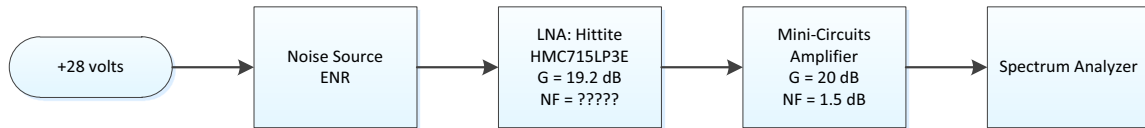


Fig. 3.3 connection diagram for noise figure measurement

$$10 * \log(Y) = N_{hot\ dB} - N_{cold\ dB} \quad (3.3)$$

$$10 * \log(F_t) = ENR_{dB} - 10 * \log(Y - 1) \quad (3.4)$$

3.3 Earlier Work Summary

This section provides a brief overview of one senior capstone project performed in the past at Bradley University, which also involves the design of a passive antenna for reception of SDARS signals.

In 2001, Greg Zomchek and Erik Zeliasz designed a front-end receiver for the SDARS [4], which includes the passive antenna design and low-noise amplifier. Also, they designed the down conversion circuitry that transformed the signal into a 70 MHz intermediate frequency ready for decoding. However, only the front-end aspect of the project was consulted as it pertained to the present project.

In this past project, Sirius ® Radio representatives and online sources were consulted and the system specifications given. These specifications were used for the present project as well, which may or may not be more sensitive than those today. For the active antenna system, the requirements for angle of reception, passive gain, and polarization are given. For the low-noise

amplifier system, the overall gain and noise figure are specified. All components must operate in the Sirius ® radio frequency band, which is between 2.32 to 2.3325 GHz.

Two types of antennas were examined in the past project: an aperture coupled patch antenna and a probe-fed patch antenna. The former was chosen because the design provides a larger bandwidth than most other feeding methods and allows amplification circuitry to be placed on the lower of two substrates making the active antenna design more compact. They introduce a method of making this design capable of receiving circularly polarized waves by perturbing the corners of the patch using [3], which is also done in the present project.

Unfortunately, it was found that slight changes in position of the aperture with respect to each layer adversely affected the bandwidth and center frequency. This made the design difficult to fabricate in-house.

Due to time constraints, a much simpler probe-fed antenna was designed and fabricated. This design needed only one substrate and kept the unperturbed, nearly-square rectangular patch. Placement of the point feed determines reception of circular polarization. This design does not allow for tuning of the input impedance after fabrication and the experimental measurement was not near the ideal $50+j0$ Ohms. However, it was shown to receive relatively circular polarization in the left screw sense with a good axial ratio. It rejected transmissions with a right screw sense, showing that the antenna can be considered left-hand circularly polarized.

3.4 Concluding Remarks

Although a probe fed antenna offers simplicity in design, it will not be feasible for an integrated antenna due to the feeding method. Components must be kept separate. The aperture coupled patch antenna is one possible option, but is difficult to fabricate. Instead, the proximity

coupled patch antenna design is the most feasible, since it offers components to be placed on the same substrate as the feedline for true integration. Proximity coupled antennas typically have higher gain and larger VSWR bandwidth.

Chapter 4 Microstrip Patch Antenna Design

4.1 Introduction

This chapter describes the initial linearly polarized patch antenna design, circularly polarized antenna design, and feedline matching circuit. All antenna designs use a proximity coupled feed. As a good stepping stone to eventually obtain a circularly polarized patch antenna design, linearly polarized (LP) design may be used to find the patch and feedline dimensions. The basis for the circularly polarized patch antenna design originated from [1], and a picture is shown in fig. 4.1.

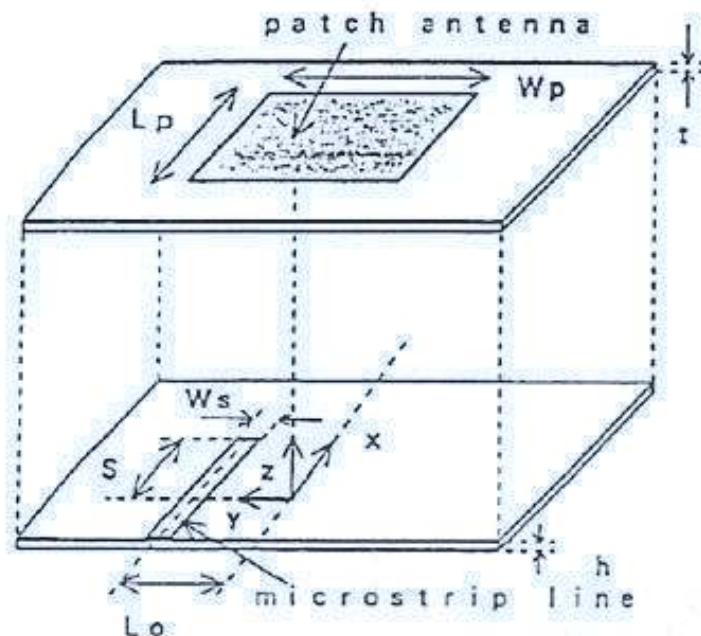


Fig. 4.1 A proximity coupled microstrip patch antenna [1]

4.2 Linearly Polarized Patch Antenna Design and Simulations

The antenna desired in this project is a microstrip antenna with a proximity-coupled feedline. Microstrip antennas have low-profile and offer simple and flexible design. The feedline accomplishes the transition between the radiating element and the port at which the LNA circuit may be connected. The feeding method was chosen to provide increased passive gain and larger bandwidth, a characteristic of proximity-coupling. There is no contact between the feedline and the radiating patch. Instead, the currents generated in the patch by EM radiation produce fields which couple to the feedline. Separation of layers also allows amplification circuitry to occupy the same substrate as the feedline, allowing for true integration of the antenna and LNA system. Separation into two substrate layers with different thicknesses also makes the design more versatile. A low dielectric constant, thick substrate for the radiating patch is used for good coupling to the feedline. The feed rests on a thinner substrate that can have a higher dielectric constant to contain the fields, reduce the size of the circuitry, and prevent coupling between components in the integrated LNA circuitry. The matching network can be incorporated into the feedline to match the impedance of the antenna to any desired impedance through use of a microstrip line matching circuit.

In fig. 4.1, the main antenna parameter names are given. These are: the length of the patch, L_p , the width, W_p , the feedline width, W_s , the feedline inset, S , and the feedline offset, L_o . S is measured from the edge of the patch and L_o from the center of the patch to the middle of the feedline. The two substrate thicknesses are represented by t and h .

In linearly polarized (LP) patch antenna design, the feedline offset L_o is zero, meaning the center is lined up with the center of the patch. L_p and W_p are calculated using the

Transmission Line Model according to [3]. Empirical equations have been derived and the length and width can be estimated given the dielectric constants, heights of the two substrates, and center operating frequency. It is notable that [3] does not account for two layered substrates that may have different dielectric constants, so equation 5 is used to calculate the combined dielectric constant used in calculation.

$$\epsilon_r = \frac{h_1\sqrt{\epsilon_1} + h_2\sqrt{\epsilon_2}}{h_1 + h_2} \quad (4.1)$$

For the substrate selection, the top substrate is to have a thickness of 125 mil and ϵ_r of 2.33. The bottom is to be 31 mil thick with an ϵ_r of 2.33. For the initial fabrication of the front-end, components were kept modular in the interest of time, so selection of a lower dielectric constant for the bottom substrate is acceptable since the LNA circuitry will be separate. In the future, a higher dielectric constant and use of (4.1) is needed.

Using these parameters, the patch length is estimated to be 1423 mil and the length 1967 mil for the width. PCAAAD 6.0 ® may be used to check the resonant frequency for the dimensions. Recreating the design in Agilent Momentum ® (see fig. 4.2), it was found that L_p is the primary determinant of the resonant frequency of the antenna. For most antenna designs, S_{11} is in the shape of an upward facing parabolic curve (see fig. 4.3). The curve minimum should occur at the center frequency of the operating range of the antenna so that the antenna is most likely to have an acceptable bandwidth after impedance matching to 50 Ohms (not performed for the LP design). Since more reliable calculations are done using Maxwell's equations instead of empirical formulas, the length was adjusted until S_{11} reached a minimum. In [1], the aspect ratio L_p/W_p was found to be 0.966. Along with L_o , the width (W_p) has an impact on circular polarization. Therefore, the width was calculated using the aspect ratio after the length was found. The new patch dimensions are $L_p = 1538$ mil and $W_p = 1592$ mil.

In fig. 4.2, the width of the feedline W_s was configured so that it had a characteristic impedance of 50 Ohms. It is necessary to do this because the LNA modules will have the same port impedance, including the researched LNA. Universal characteristic impedance is helpful in matching port impedances so that there is maximum power transfer between devices. The inset length S was found to have a very large impact on the imaginary part of the impedance at the passive antenna port, so it was adjusted until there was none. Doing this could shorten the matching circuit needed to convert the antenna impedance to 50 Ohms. The feed inset also has an impact on the amount of coupling between the feed and the patch, so the inset could also be adjusted to get the largest impedance locus (on a smith chart), also aiding in impedance matching. A larger impedance locus could produce a better match to 50 Ohms, which makes matching network design easier and less sensitive to changes in dimensions. For now, the zero imaginary impedance method was used and $S = 814$ mil, but it is worth investigating the coupling in a later project.

In fig 4.4, the gain of the LP antenna was simulated to be a robust 6.4 dB. Fig 4.5 shows the simulated axial ratio. This is measured through differences in reception of LHCP and RHCP waves. The high axial ratio shows extreme linear polarization.

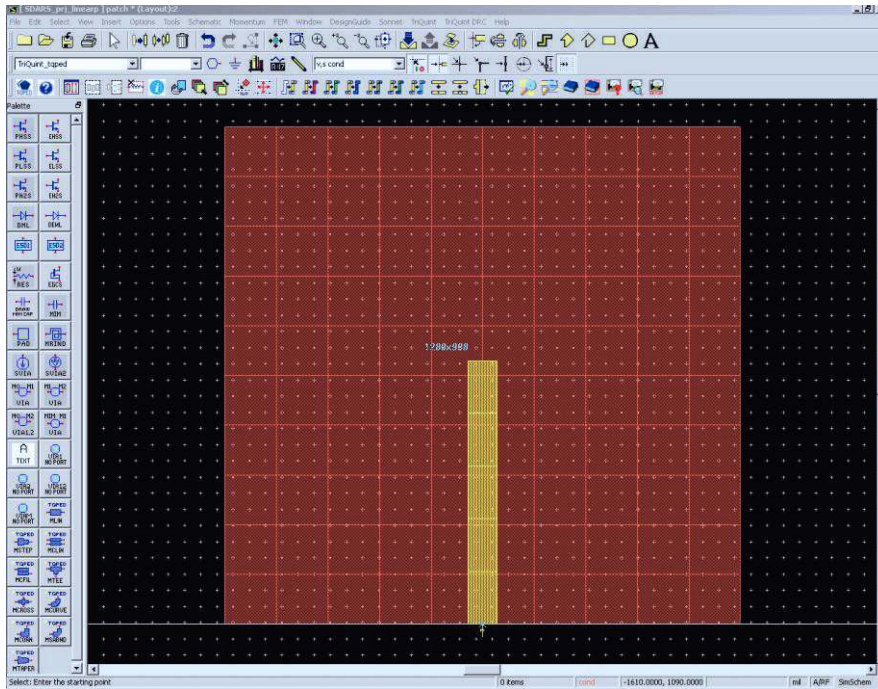


Fig. 4.2 LP patch design in Momentum ®. Red = upper layer, yellow = bottom layer

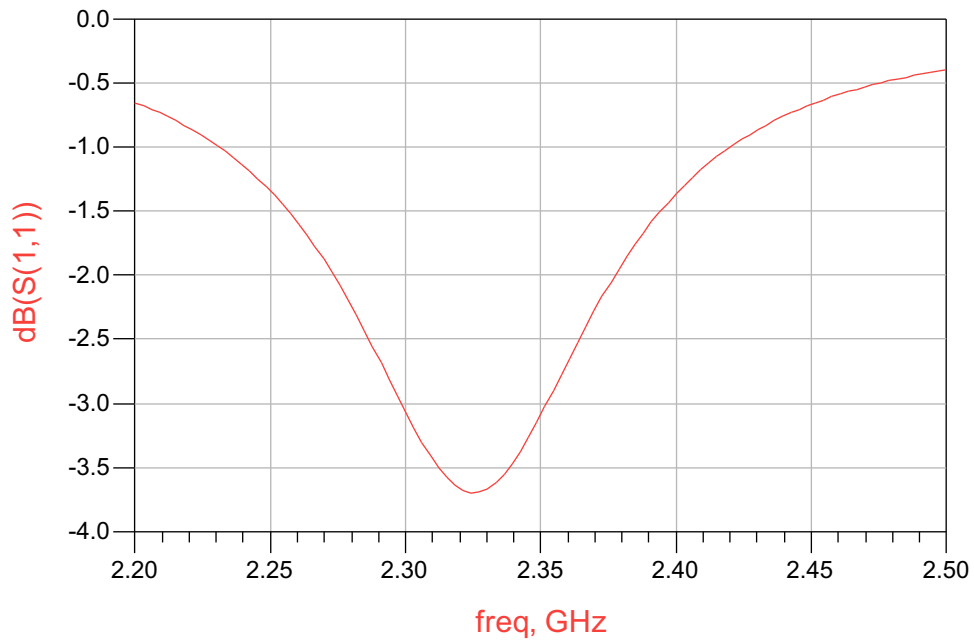


Fig. 4.3 Momentum ® simulation of $|S_{11}|$ vs. frequency for the LP design

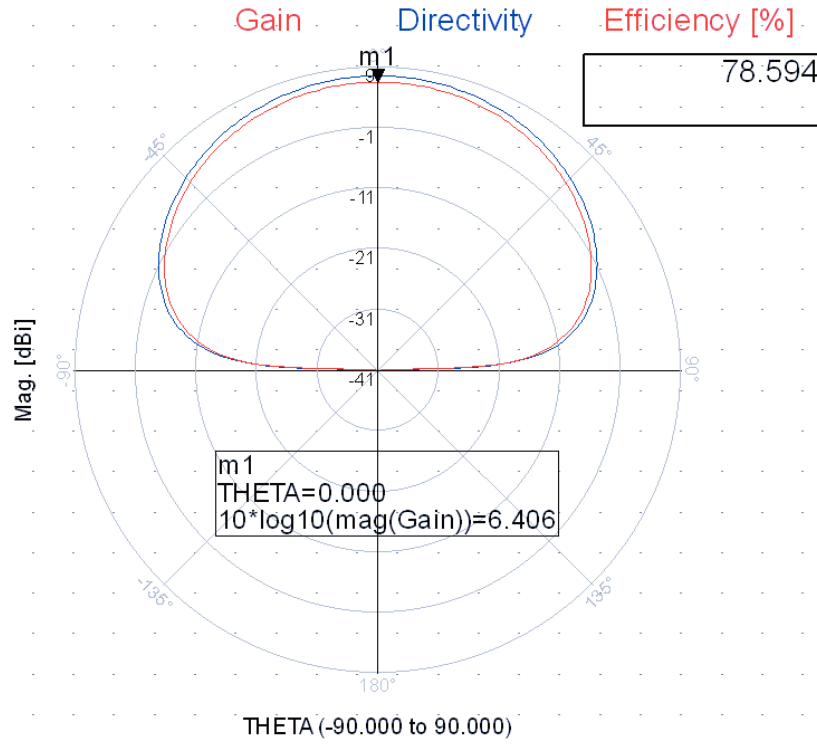


Fig. 4.4 LP antenna gain simulation in Momentum ®

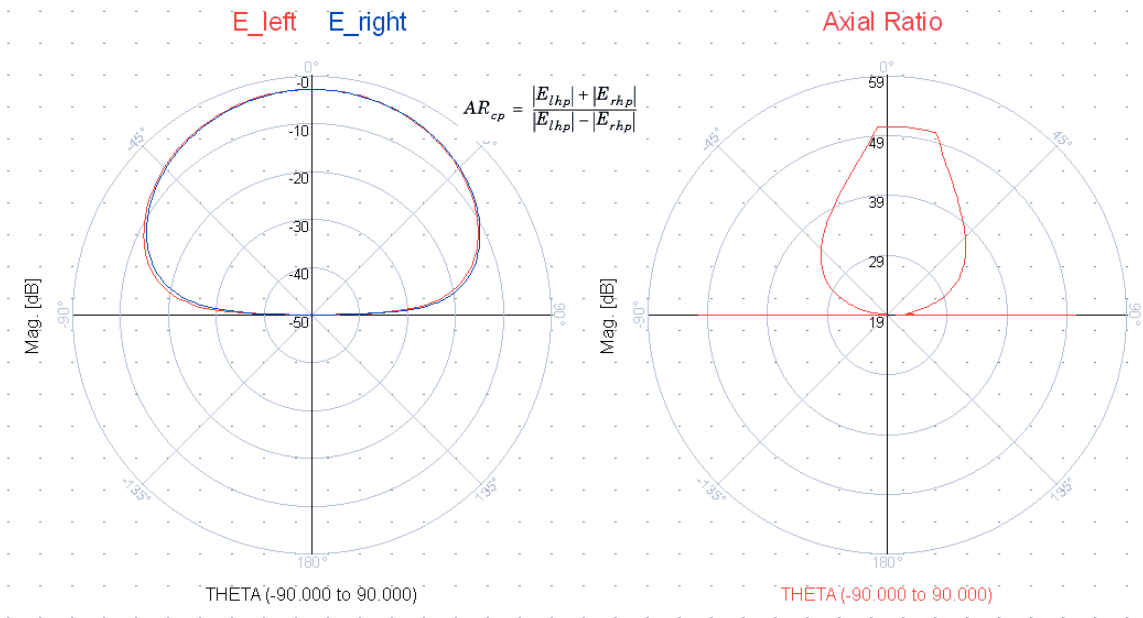
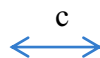


Fig 4.5 Momentum ® simulation of LP antenna axial ratio (shows high linear polarization)

4.3 Circularly Polarized Antenna Design and Simulations

From [1], a linearly polarized patch antenna with a proximity-coupled feed can be made circularly polarized (CP), simply by adjusting the feedline offset L_o away from the center of the patch. The authors show that they have obtained an axial ratio (AR) of 0.8 dB by adjusting the patch width W_p and L_o . It was found in simulations that the line inset S does not have a significant effect on the AR. Refer to appendix A for extensive measurements. Table A1 shows that the lowest AR occurs when the feedline is near the edge of the patch with a long inset. Since the AR could not be simulated to be below 3 dB by changing all other geometrical parameters except for the substrate thicknesses and dielectric constants, a new design was considered.

In [6] and [7], a method to perturb the rectangular patch in opposite diagonal corners is given, which helps to separate the orthogonal modes and allow for CP. Refer to fig. 4.6 for a diagram. The Patch dimensions from the LP design were maintained. The length c indicates how much the patch is perturbed from its original rectangular shape. Perturbations must occur at these corners to receive left-hand circularly polarized (LHCP) waves, while modifications at the other corners will make the antenna right hand circularly polarized (RHCP). From (6), the amount of area ($s = L_p * W_p$, and $\Delta s =$ total perturbed area) to perturb is based on the unloaded quality factor of the antenna, which is a measure of losses associated with the dielectric material, conductivity of copper, and radiation losses (see (7)). In fig 4.6, $c = \text{sqrt}(s)$. Using (6) through (10), the total perturbed area is 68092.67 mil^2 , making $c = 260.94 \text{ mil}$. This provides a good starting point in Agilent Momentum ®, in which c was optimized to 285 mil to obtain the lowest simulated axial ratio. It was observed that the axial ratio was adversely affected with any change in the feedline offset, L_o , so it was moved back to the center of the patch.



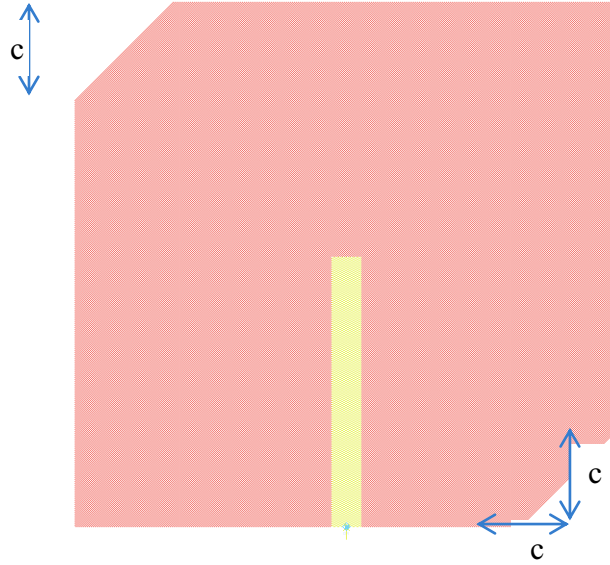


Fig 4.6 Perturbed CP Patch Antenna. Red = upper layer, Yellow = lower layer.

$$\frac{\Delta s}{s} = \frac{1}{2Q_o} \quad (6)$$

$$\frac{1}{Q_o} = \frac{1}{Q_{rad}} + \frac{1}{Q_c} + \frac{1}{Q_d} \quad (7)$$

$$Q_c = h\sqrt{\pi f \mu_o \sigma} \quad (8)$$

$$Q_d = \frac{1}{\tan \delta} \quad (9)$$

$$Q_{rad} = \frac{3\epsilon_r}{8} * \frac{\lambda_o}{h} \quad (10)$$

Using the parameters described above, simulations in Momentum ® were performed. The results are shown in figs. 4.7 through 4.10. In the return-loss measurement, resonant frequency has shifted away from the target center frequency. However, the patch still radiates somewhat because S11 is lower than 0 dB, or the signal is not completely reflected. We can compensate for this by designing a matching network for the antenna so that S11 is less than -10 dB in the target band (VSWR < 2). From the Smith chart, the unmatched antenna port impedance is much lower than that of the LP design. For the LP antenna, the real impedance at the center frequency was 10.5 Ohms. The perturbed patch had a simulated real impedance of 3.6 Ohms. Such small

impedance requires large lengths or widths of the microstrip line matching circuit (depending on the type used). This also increases sensitivity to changes in the geometric parameters of the network. If lumped-element components are used, they must also be precise. This could make production of this type of antenna difficult. The axial ratio passes the less than 3 dB specification at the center frequency, and was found to improve toward 2.32 GHz and push the specification near 2.3325 GHz. The gain remains relatively constant after transitioning from the LP design.

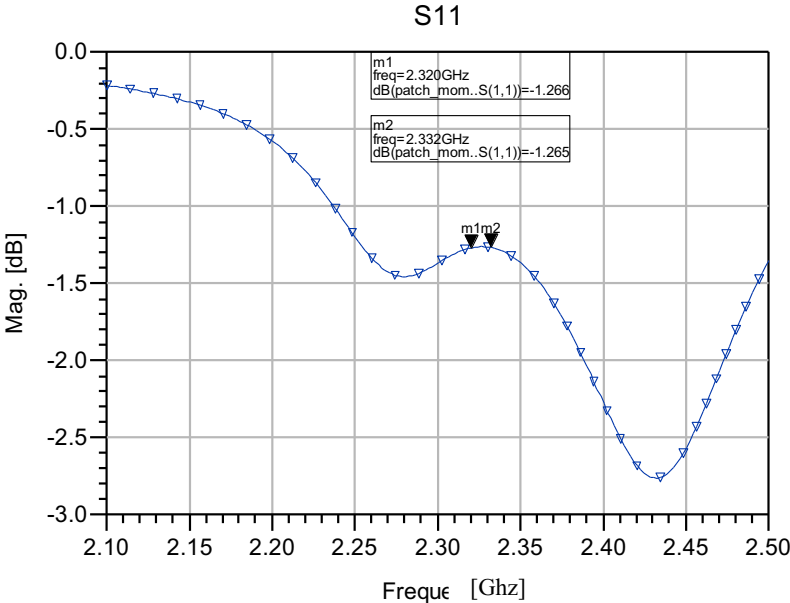


Fig. 4.7 |S11| simulation of perturbed patch antenna

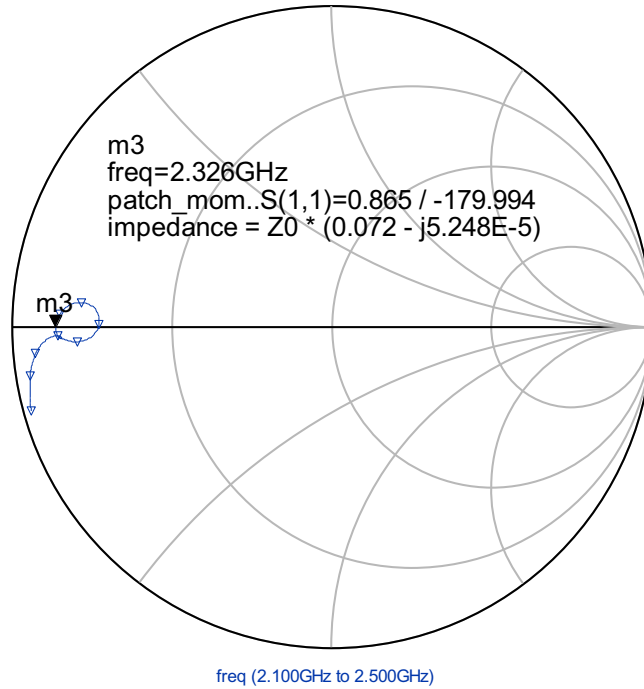


Fig. 4.8 Simulated Z_{in} of the perturbed patch antenna

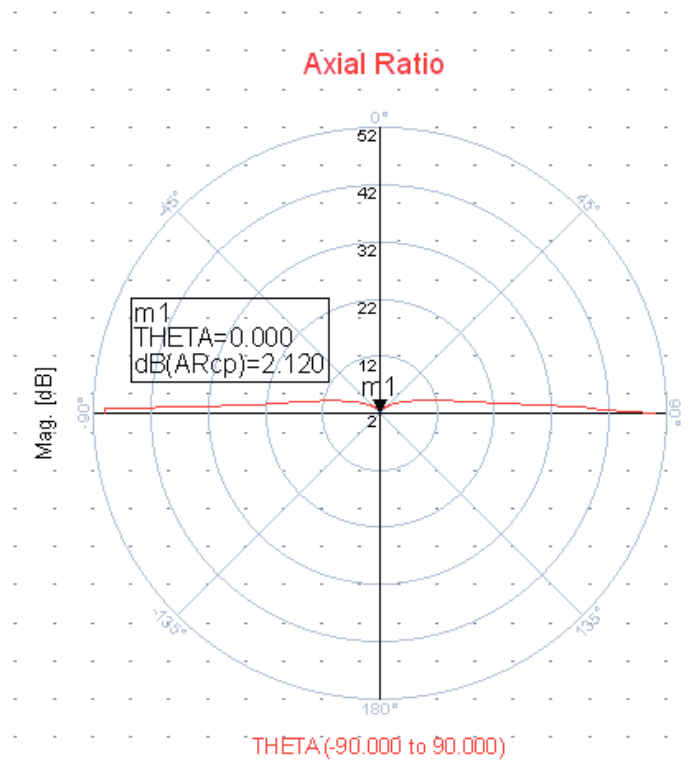


Fig. 4.9 Simulated axial ratio of the perturbed patch antenna

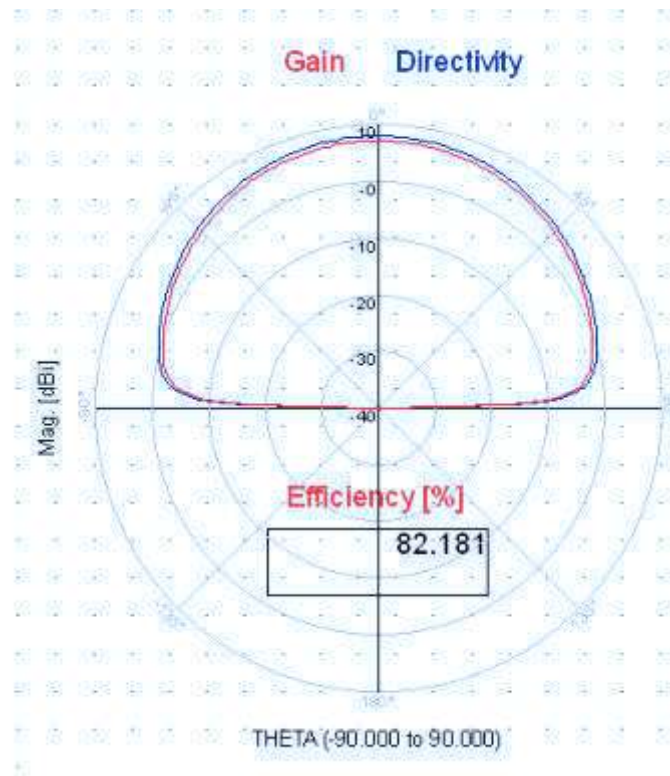


Fig. 4.10 Simulated gain of perturbed patch antenna

4.4 CP Antenna Feed Line Matching Network

Since the patch dimensions were finalized and the input impedance over the operating frequency range was obtained using Momentum [®], a matching circuit was designed using [5] in order to meet the VSWR specification. The matching network ensures maximum intercepted power is transferred to the LNA circuitry. Among the options for transforming the low 3.6 Ohm antenna impedance to 50 Ohms includes single-stub matching network, quarter wave transformer, or lumped element network. It was determined that only a single-stub matching network could be used to make the design as low-profile as possible. Because the impedance is so low, both quarter-wave transformer options are not feasible. One used a very wide transmission line, which may radiate undesirably. The other used an extremely thin microstrip line, which could not be fabricated. Even though a lumped-element network takes up the smallest

space, the impedance is so low that tolerances of inductors or capacitors must be very low, which could drive up production costs. Therefore, the single-stub matching network was used. See fig. 4.11 depicts the design. The width of the microstrip line corresponds to a characteristic impedance of 50 Ohms and is the same width as the antenna feed. A length of 1424 mil from the passive antenna port to the T-junction and an open-stub length of 1039 mil were required to match the antenna. The length of the line from the T-junction to the LNA network port was included so the SMA connector could be soldered on the feed in the final stages of fabrication. In order to keep the size of the substrate within the limit imposed by the fabrication equipment (spin coater), meandering of the microstrip line was necessary.

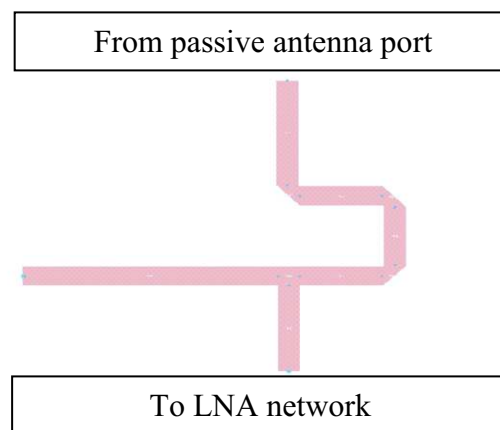


Fig. 4.11 Single stub matching network for the CP patch

Including the feedline with the antenna in design simulations, adjusted S11 and the feedline input impedance may be obtained. See Appendix C for the ADS ® schematic. See fig. 4.12 for S11 and fig 4.13 for input impedance. For S11, the return-loss is shown to greatly improve and meet the VSWR specification within the target band.

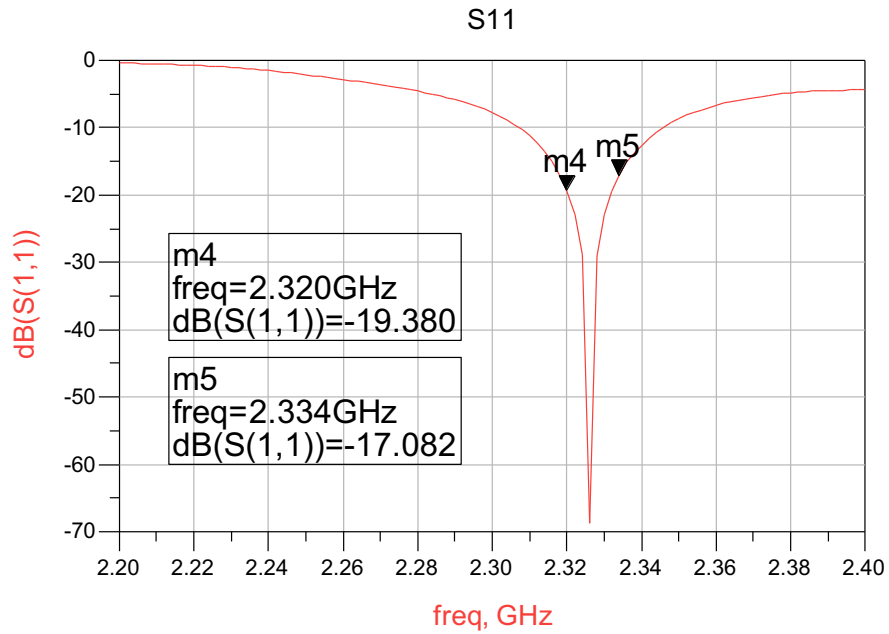


Fig. 4.12 |S11| measured at the matching network port

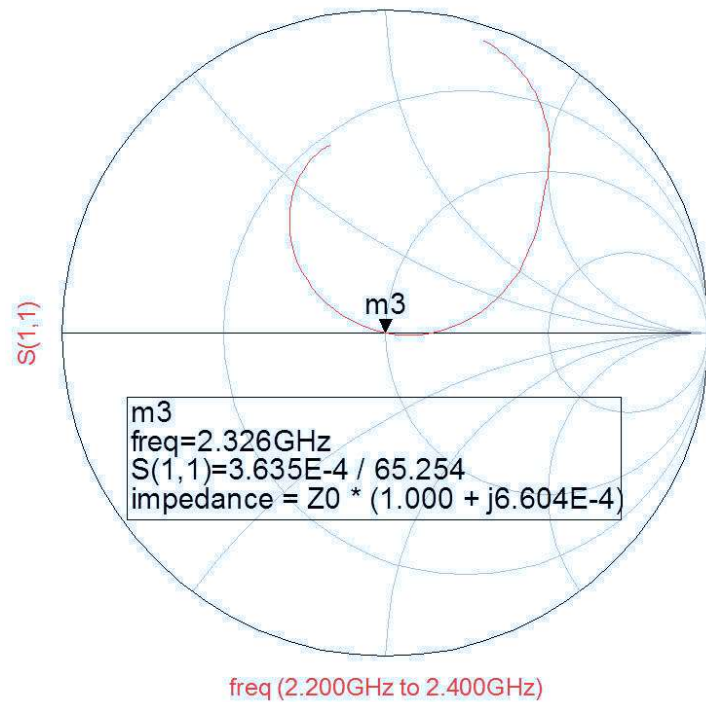


Fig. 4.13 Input impedance measured at the matching network port

4.5 Concluding Remarks

When the linearly polarized patch antenna was converted to a circularly polarized one, the center frequency was shifted upwards slightly. The matching network was relied upon to correct this shift and bring the S11 minimum back to the center frequency. The VSWR was improved to meet the SDARS specification in the target frequency band.

Chapter 5

Circularly Polarized Antenna Fabrication and Measurements

5.1 Introduction

This chapter describes the antenna fabrication process, including details about some difficulties that were encountered. With materials for four possible antennas, only one could be considered acceptable for measurements. Measurements of S11, input impedance, gain, and axial ratio were performed. The antenna beam pattern and test for LHCP was not measured due to a lack of a standard left-hand circularly polarized antenna for use in the lab at the time.

5.2 Antenna Fabrication

The fabricated antenna is shown in fig. 5.1. The fabrication of two parts of the antenna (feedline and patch) was done using the step-by-step instructions and the PCB board fabrication equipment available in the MIC fabrication facility. The PCB boards are first cut into 9.45 cm by 9.45 cm squares so that they may be secured on the spin coater, a device used to spread the photoresist chemical solution in the first stages of fabrication. After fabrication, the two laminates were pressed together using a fast drying adhesive. Places where the photoresist did not get applied evenly caused unwanted removal of copper. Therefore, solder was used to repair these holes. Unfortunately, there were some breaks in the feedline that had to be soldered, which

can affect the input impedance. There were enough materials to build four antennas, but only one could be constructed successfully and used in measurements without major imperfections.

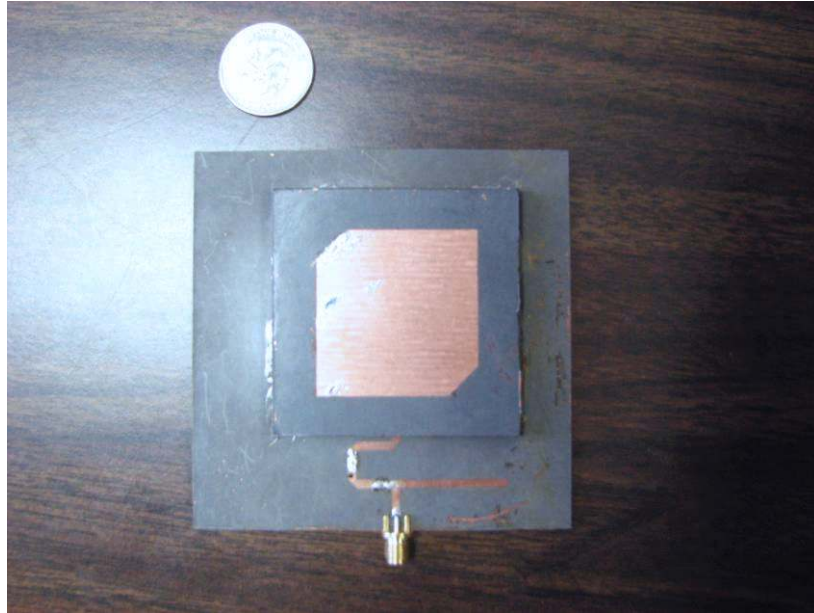


Fig 5.1 Fabricated perturbed patch antenna with matching circuit

5.3 Antenna Measurements

Using the network analyzer, S_{11} and the input impedance were measured at the SMA connector of the antenna (see fig 5.2 for the measurement setup). See figs. 5.3 and 5.4 for the measured results. The center frequency has shifted from the desired band and the antenna does not meet the VSWR specification. This could be due to the solder introduced on the patch and feed network or shifted placement of the top substrate on the lower substrate. One critical error in fabrication was that the antenna patch mask was flipped upside down. This switched the length and width of the patch relative to the feedline. Now, the length is actually longer than desired by 54 mil. This should shift the center frequency downward, but an increase is observed instead. Because the length is longer, the feedline inset relative to the patch edges is also changed. This might have changed the input impedance of the antenna before the matching

circuit. The matching circuit could be performing its function, but the starting impedance has changed, thus changing the impedance at the output. There is a good chance that the return loss is affected by an impedance mismatch, resulting in fig. 5.3.



Fig. 5.2 Measurement setup of S11

The axial ratio was measured in the anechoic chamber. The measured value was increased greatly because of this critical error. Refer to appendix D for this measurement. The width of the patch has a large effect on the axial ratio, which is now 54 mil shorter than desired. The axial ratio was measured to be 27.94 dB!

Using the Friis transmission formula and the known gain of a LP standard antenna, the gain of the fabricated antenna was measured to be 5.8 dB. This value reasonably matches the gain predicted in simulation.

Since a standard LHCP antenna is not presently available in the lab when measurements were taken near the end of the semester, the fabricated antenna beam pattern and LHCP test could not be performed.

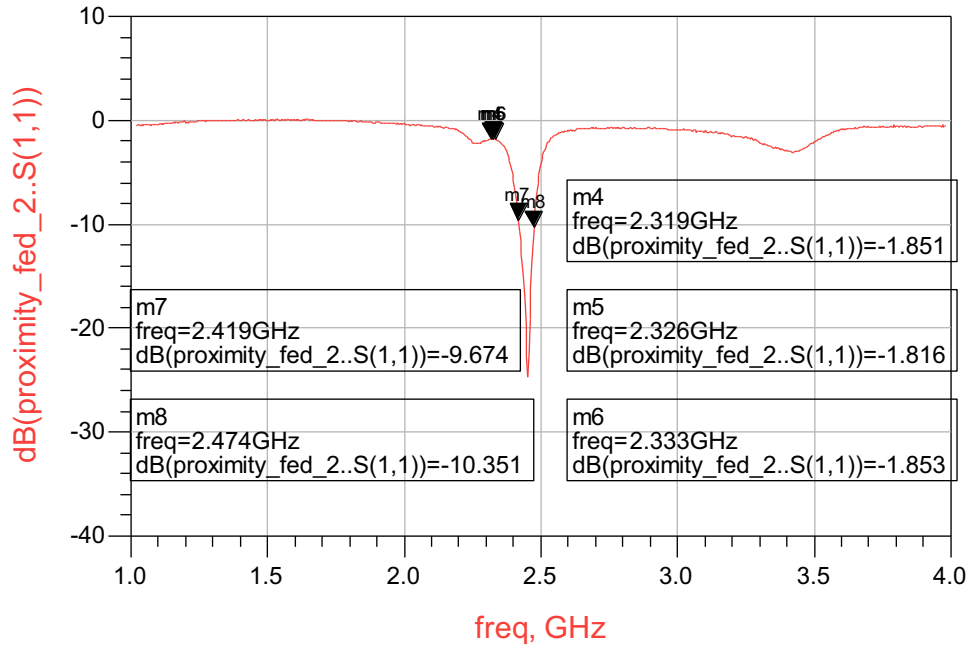


Fig. 5.3 Measured $|S_{11}|$ of the fabricated antenna

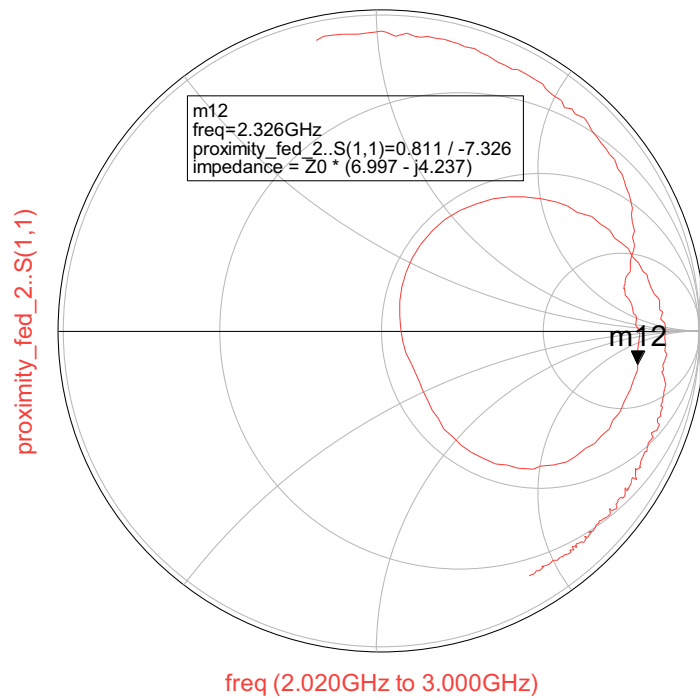


Fig. 5.4 Measured input impedance of fabricated antenna

5.4 Concluding Remarks

Due to misplacement of the antenna patch mask and imperfections in fabrication of the antenna, the measured results differ greatly from the simulated measurements. Correction of the

flipped antenna mask during fabrication and accurate placement of the feedline should provide improvement. Any future design should be outsourced for a more precise fabrication process.

Chapter 6 **Low-Noise Amplifier Subsystem**

6.1 Introduction

This chapter includes a complete functional description, component selection, and testing of the low-noise amplifier (LNA). In the interest of time, the LNA component of the front-end is kept modular. In the future, integration with the passive antenna is possible by including the amplifiers on the same substrate as the feed and matching port impedances between the antenna and LNA.

6.2 LNA subsystem

Research of a surface mount package led to the discovery of Hittite Corporation's HMC715LP3E low-noise amplifier. See appendix E for the data sheet of the amplifier. It has a 19 dB gain and a 0.9 dB noise figure. The noise figure approaches the maximum specified value, but LNA options were limited and few surface mount packages offered port impedances pre-matched to 50 Ohms. Cascading two of these will meet the gain specification. Hittite has provided an evaluation board with its port impedances almost matched to 50 Ohms, but slightly off due to the inclusion of blocking capacitors at the input and output. Using this board and a Mini-Circuits Corporation ZEL-1724LN amplifier (see appendix E for the data sheet) provides a temporary means to test the fabricated antenna with the Sirius[®] radio receiver, the ultimate goal of the project (see fig. 6.1). We can use an amplifier with an arbitrary noise figure at the second stage because total contribution of noise is primarily contributed by the first. A cascaded LNA

system may be powered by the radio receiver itself in the future when the LNAs are on the same substrate as the feedline.

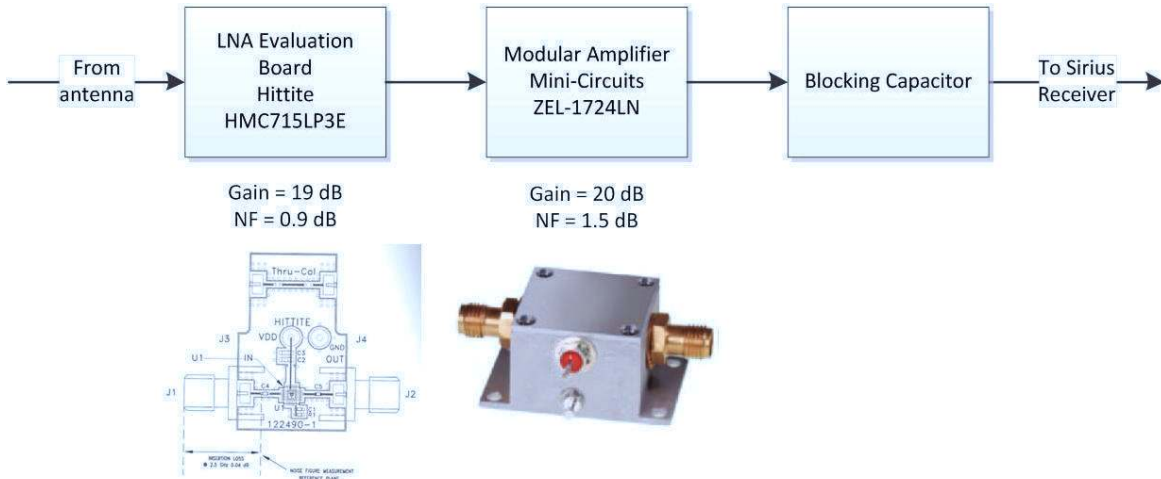


Fig. 6.1 Block diagram of LNA subsystem

6.3 LNA measurements

The Hittite LNA was tested for gain using the network analyzer, and it has a 19.2 dB gain. The noise figure of the LNA and for the total amplifier system can be obtained using a spectrum analyzer and a noise source, shown in fig. 6.2. Calculations are sensitive to any changes in the recorded noise power when the noise source is off and when it is on and the averaged noise power displayed on the spectrum analyzer would fluctuate as much as 2 dB. Therefore, the overall noise figure of the system was measured to be between 1.38 and 4.57 dB. A method of obtaining a statistical running average of measurements would have been a useful tool to have, which might provide better accuracy. It was found that the contributing noise factor by the second stage was 0.005, so the overall noise figure approximates the noise figure contributed by the first stage.

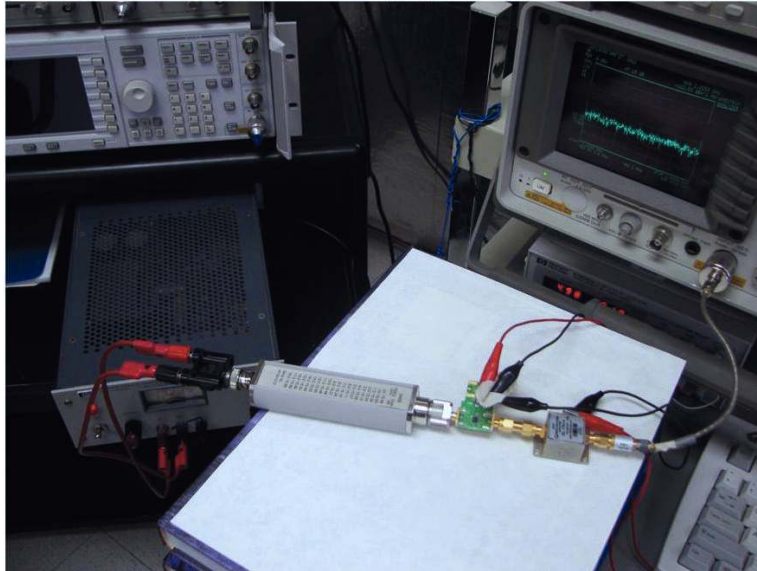
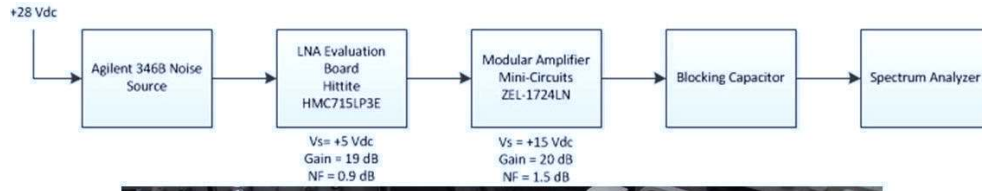


Fig. 6.2 LNA noise figure measurement setup

6.4 Concluding Remarks

The Hittite amplifier was measured to have a gain that matched specifications and a slightly higher noise figure most likely due to the added blocking capacitors on the Hittite evaluation board. The PCB board design and fabrication needed to mount the individual HMC715LP3E chips were not complete.

Chapter 7 SDARS Front-End Testing and Post-Fabrication Simulations

7.1 Introduction

This chapter describes the Front-End test with the Sirius ® Receiver and post simulations. Measurements of actual antenna parameters were taken as accurately as possible and used them in the respective parameters of the design in Agilent ADS ® in an attempt to model the observed, major changes in the fabricated antenna characteristics.

7.2 SDARS Front-End Testing

The SDARS front-end was assembled as shown in fig. 7.1. A blocking capacitor is placed at the output to protect the LNA components from the 5-volt DC supply of the Sirius[®] Receiver. Both amplifiers must be powered separately. Fig. 7.2 shows the front-end connected to the Sirius[®] receiver and fig 7.3 shows it connected to the spectrum analyzer. With the front-end attached, the receiver was able to produce an audible signal with a standard pair of stereo speakers.

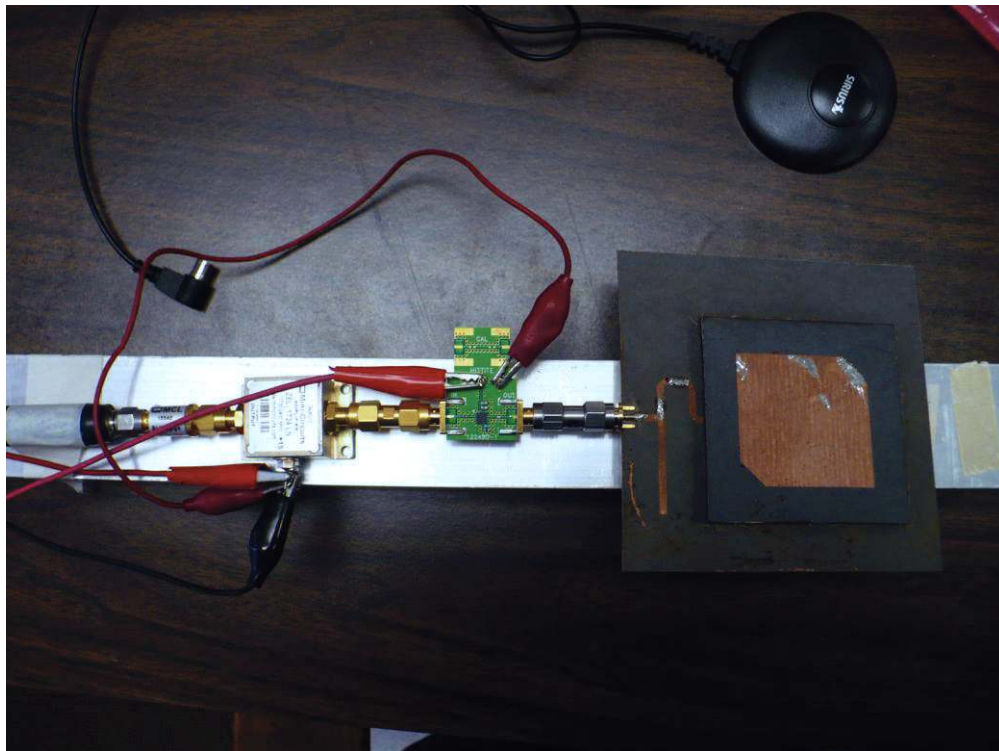


Fig 7.1 Front-End



Fig 7.2 Front-End connected to the Sirius ® Receiver

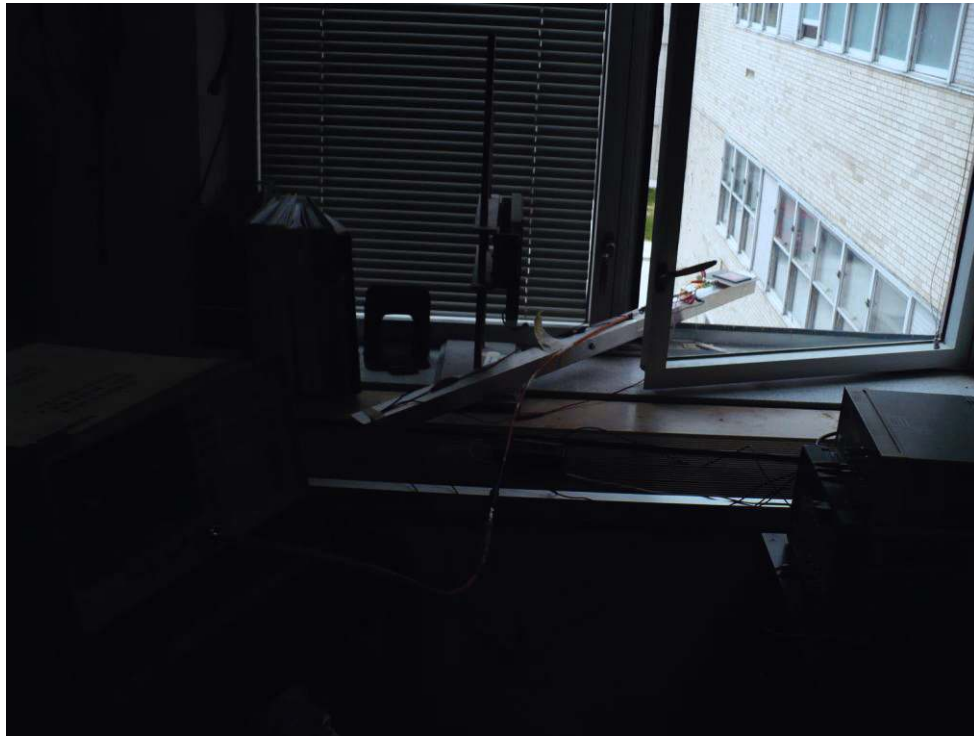


Fig 7.3 Front-End connected to Spectrum Analyzer

7.3 Post-Fabrication Simulations

An explanation of measured results of the antenna is needed to see what happens when the mask was turned over or placement of the feedline is adjusted when the two substrates were glued together during fabrication. In an effort to reproduce a simulation that would explain the changes seen in the measured results, physical measurements of the patch dimensions were taken and inserted into Momentum ®. See table 7.1 for parameter changes. The feedline width and matching circuit are kept the same in the simulation to isolate the affects from changes in the patch orientation and placement.

Table 7.1
Physical measurements of changes in the patch dimensions

Parameter	measure [mil]	change from design [mil]
S	835	66
Wp	1532	-60
Lp	1583	45
Lo	13	right 13

As seen in figure 22, the resonant frequency of the antenna and matching network has shifted to 2.34 GHz, outside the target band. Similarly from measured results, we saw an increase to 2.45 GHz. This is primarily due to the feedline inset adjustment, which can change the input impedance of the antenna. To help explain the increase in axial ratio, fig. 7.2 places it at 10 dB, which is still shy of the measured 30 dB! The feedline was also offset to the right by 13 mil. This could have contributed to the increase in axial ratio, and new locations for the patch perturbations could have contributed to that as well.

The feedline changes were also taken into consideration, in that the models for the 90 degree bends and tee-junction could have increased the length of the lines during the transfer to a printable layout. However, an increase in the lengths has caused severe changes away from the

measured results, so the feedline may be performing its function. It is useful to see what happens as the length of the open stub of the matching network is varied. When increased, the center frequency is shifted downward. Decreasing shifts the center frequency upward.

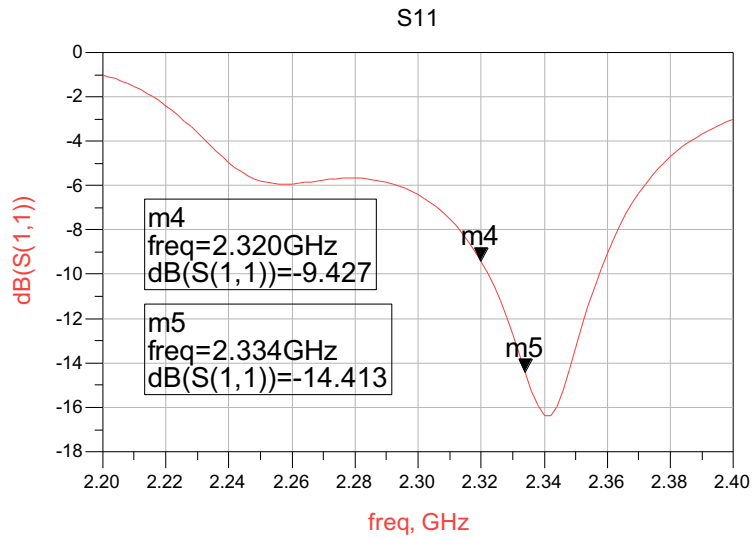


Fig. 7.1 Simulated $|S_{11}|$ measured at the matching network output with changes in patch dimensions

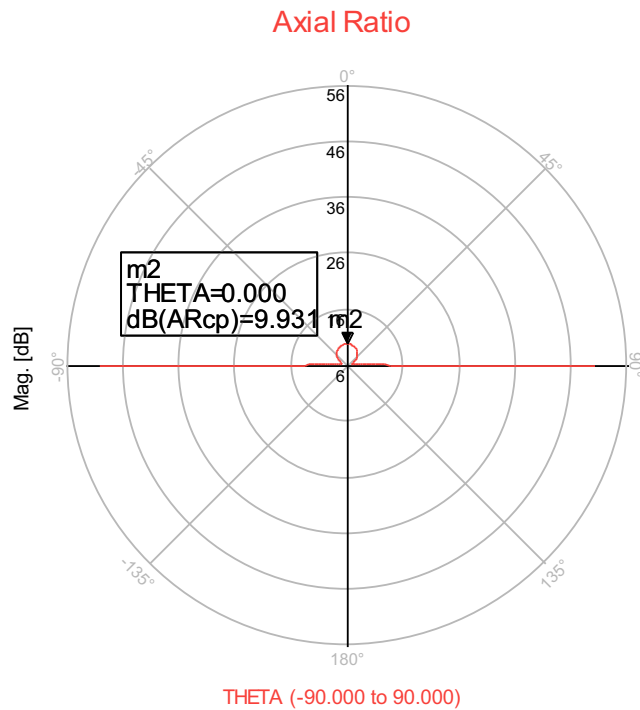


Fig. 7.2 Simulation results of axial ratio using changes in patch dimensions

7.4 Concluding Remarks

The simulated results in figs. 7.1 and 7.2 correspond to changes in the patch dimensions only, modeling an upside-down patch layer. Increased axial ratio was observed, but not to the 30 dB magnitude measured in lab. The feedline could be not centered under the patch, which was simulated to show adverse affects on axial ratio. Any changes in the feedline matching circuit had degraded antenna performance beyond even what was measured.

Chapter 8 Conclusions and Suggestions

In conclusion, one proximity-coupled, perturbed patch antenna was fabricated and tested for VSWR, axial ratio, gain, and input impedance. Due to errors in fabrication, the VSWR and axial ratio specifications were not met. Running a simulation to include the mistake will prove useful in determining if it is a design issue or a fabrication issue. If the simulation gives similar results to the ones measured, then it is a fabrication issue.

The low-noise amplifier system was kept modular in the interest of time, but a PCB to place the HMC715LP3E surface-mount packages can be designed for placing the amplifiers on the same substrate as the feed in the future. Selecting a higher dielectric constant substrate for the feedline is necessary for future integration, and the size of the patch may also be reduced by choosing a higher dielectric constant substrate.

When attempting to model the errors made in the fabrication process, simulation results approach measured results for S11 and axial ratio in some respect, but could not be exactly reproduced. Placement of the mask right side up would have improved these parameters to desired specifications.

Even with the antenna out of specification and the increased LNA noise figure, music could be played from the Sirius ® receiver when the front-end was connected to it. This could be due to the high received power and receiver gain or increased sensitivity of the receiver (since 2001). The specifications were also taken from 2001, so they may be more stringent than they are now! When the front-end is placed outside the window and connected through a long coaxial cable to the spectrum analyzer, increased power within the operating frequency range was observed. The front-end is proven to perform its function.

References

- [1] H. Iwasaki, H. Sawada, K. Kawabata. "A Circularly Polarized Microstrip Antenna Using Singly-Fed Proximity Coupled Feed." Institute of Electronics, Information and Communication Engineers. September 1992. pp. 797-800.
- [2] J.R. James, P.S. Hall, C. Wood. Edited by G. Millington, E.D.R. Shearman, J.R. Wait. *Microstrip Antenna Theory and Design*. The Institute of Electrical Engineers, London and New York. Peter Peregrinus Ltd., 1981.
- [3] Balanis, Constantine A. *Antenna Theory: Analysis and Design*. 2nd Ed. John Wiley and Sons, Inc., 1997. pp. 760-762.
- [4] Greg Zomchek, Erik Zeliasz. *SDARS Front-End Receiver: Senior Capstone Project Report*. Advised by Dr. Prasad Shastry. ECE Dept. Bradley University May 13, 2001.
- [5] Ulaby, Fawwaz T. *Fundamentals of Applied Electromagnets*. 5th ed. Pearson Education, Inc. 2007.
- [6] Sainati, Robert A. *CAD of Microstrip Antennas for Wireless Applications*. Artech House, January 15, 1996.
- [7] James R. James, Jim R. James, Institution of Electrical Engineers. *Handbook of Microstrip Antennas* Vol. 2. Peter Peregrinus Ltd. 1989. pp. 228-231.
- [8] Kazuhiro Hirasawa, Misao Haneishi. *Analysis, Design, and Measurement of Small and Low-Profile Antennas*. Artech House, Boston, London.

Table A2

Simulation AR as a function of W_s and W (no significant changes)

Lo = 696.5	S = 1384.2	W = 1592	L = 1538		Lo = 696.5	S = 1384.2	Ws = 70	L = 1538
Ws	axial ratio (dB)				W	axial ratio (dB)		
50	8.117				1630	9.175		
60	7.993				1620	8.693		
70	7.948				1610	8.277		
80	7.954				1600	7.994		
89.25	7.971				1592	7.948		
95	7.982				1585	8.095		
100	7.992				1580	8.36		
110	8.012				1575	8.793		
120	8.034				1570	9.424		

Table A3

Simulation gain as a function of W_s and S of the perturbed patch design (no significant changes!)

L = 1538	W = 1592	c = 285									
Ws \ S	100	200	300	400	500	600	769	800	900	1000	1100
30							6.438				
40							6.488				
50							6.527				
60							6.563				
70	6.119	6.348	6.46	6.522	6.559	6.582	6.592	6.591	6.573	6.53	6.443
80							6.614				
89.25							6.627				
100							6.639				
110							6.649				
120							6.658				
130							6.666				

Table A4

Axial ratio vs. frequency for the final perturbed patch design

freq	AR (db)
2.32	1.742
2.322	1.873
2.324	2.033
2.326	2.216
2.328	2.414
2.33	2.627
2.332	2.855
2.334	3.086

Appendix B

Printing Designs in ADS for Technicraft Corporation

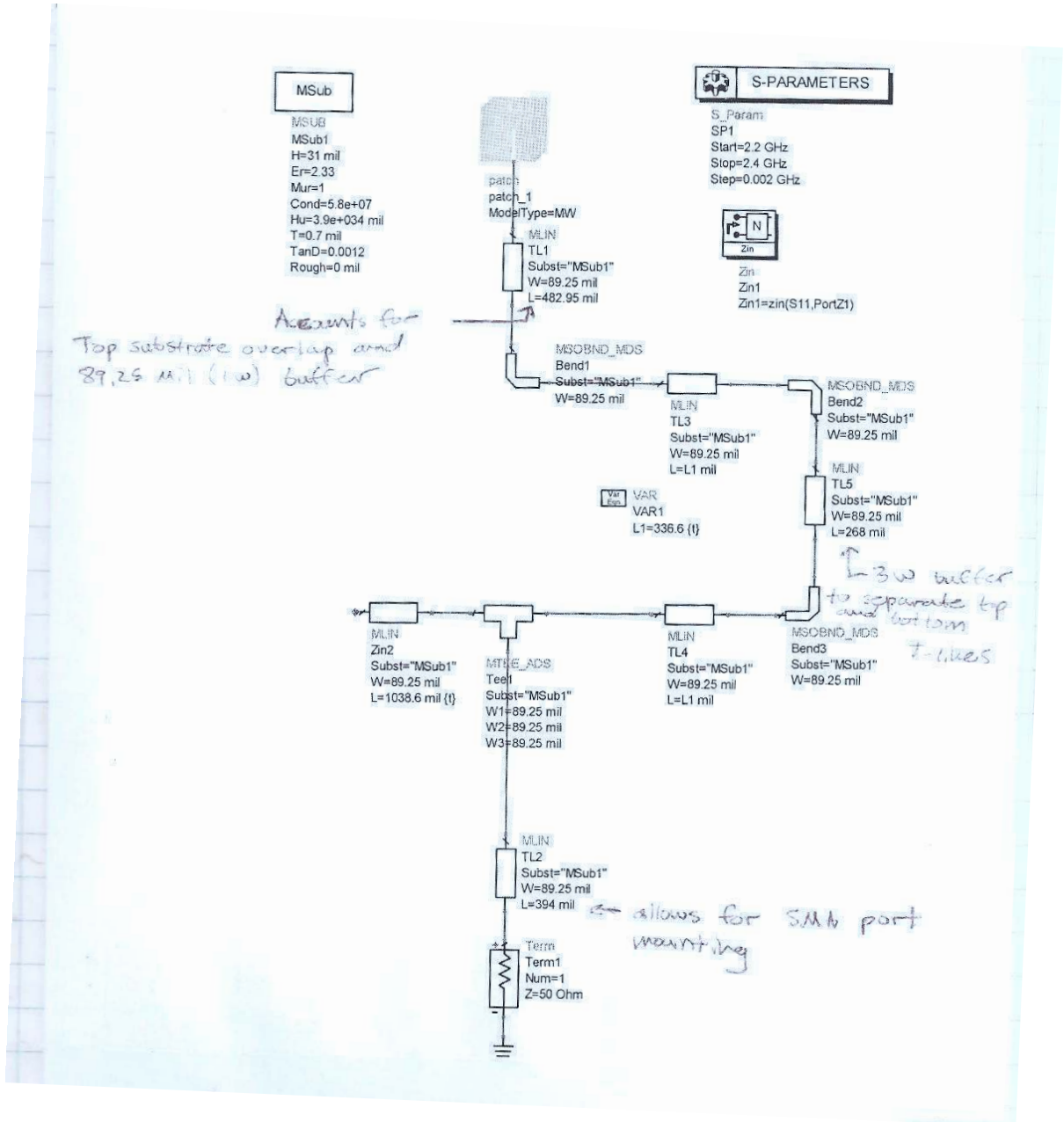
The following are updated (2011) instructions for getting .eps and .pdf of your design using ADS. This process is used in the creation of masks, which are necessary in the printed circuit fabrication process. The file formats conform to the requirements of the company *Technicraft* that produces these masks.

1. If your design is in the schematic screen, transfer your design to the layout screen by clicking **Layout → Generate/Update Layout...**, make any adjustments to your liking in the Generate/Update Layout dialog box, and click ok.
2. In the layout screen, you will see the physical equivalent of your circuit in the schematic screen, including all the labels and node points. You must get rid of unwanted symbols and text before beginning the .eps and .pdf file creation process. Refer to the second half of page 12 of *ADS Tutorial Manual (Part-I)* before proceeding further.
3. Ensure your drawings fit in a standard 8.5"*11" sheet by using the measurement tool under **Insert → Measure...** And measure a box with a maximum of 7.5"*10" (one inch margins) that encompasses your layout.
4. With the text and symbols removed, click **File → Print Area** and create the same box as in step 3. The Print dialog box appears. Change the printer name to *Generic PostScript Printer*. If this option is not available, contact Chris Mattus. **UNCHECK THE BOX "Fit to Page"** in the lower left-hand corner so that your drawing prints to scale. Click ok.
5. The Print to File dialog box appears. Type *filename.eps* and click ok. The created file is located in your project folder. Move the file to H:\Temp. Leave your workstation and log into one of the computers in the IEEE lounge room 242, which have a necessary program called Acrobat Distiller. Find your .eps file in H:\Temp and change the file extension to *filename.ps* and double click on it, which should automatically open Acrobat Distiller and process your file into a .pdf. This .pdf file is created in the same directory as the .ps file.
6. Open the .pdf file and print to one of the LaserJet printers. **PHYSICALLY MEASURE YOUR DESIGN** to make sure it actually matches dimensions in ADS.
7. Collect the .eps and .pdf files and save them in a safe place. These files may be transferred to *Technicraft* Company. They will automatically darken your design to be pitch black (as opposed to grey). When talking to *Technicraft*, you want **linotype 8.5"*11" sheets**. Specify **positive** (your objects are dark and the surroundings clear), **emulsion down** (your design may not be scratched off the sheet), **100% pitch black** (your design is completely black, necessary for fabrication at BU).
8. When picking up your masks from *Technicraft*, physically measure the linotype sheets again to ensure accuracy.

Technicraft Company
419 Elm Street or 7930 N. University Street
Peoria, IL
61605
*309 - 495 - 5245
309 - 691 - 4432
www.technicraft.net

Appendix C Perturbed Patch Antenna and Final Matching Network

Fig. C1 Perturbed patch microstrip antenna model and connected microstripline matching network in Advanced Design System ®. Total design is confined to a 9.45 cm x 9.45 cm square for fabrication



Appendix D Measurement of Axial Ratio in Anechoic Chamber

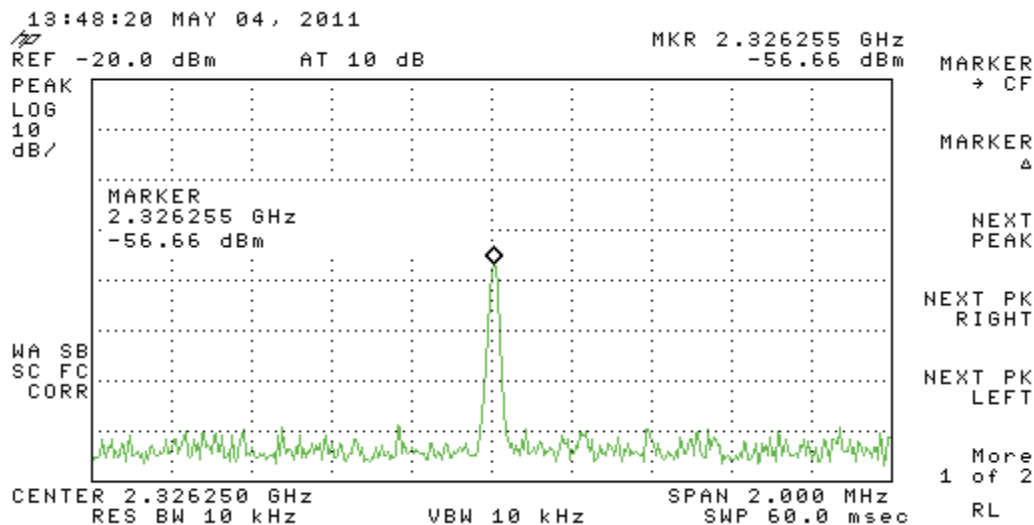


Fig. D1 received power with the antenna oriented upright in the anechoic chamber

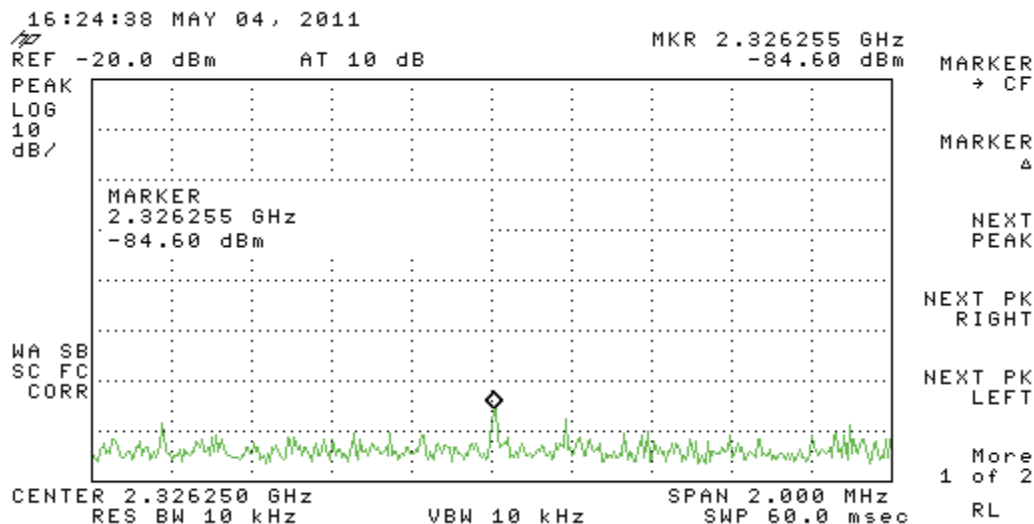


Fig D2 Received power with the antenna turned 90 degrees on its side (patch still faces transmitter).

Appendix E
Data Sheets

Hittite Corporation's Low-Noise Amplifier
HMC715LP3E

Mini-Circuits Low-Noise Amplifier
ZEL-1724LN



Typical Applications

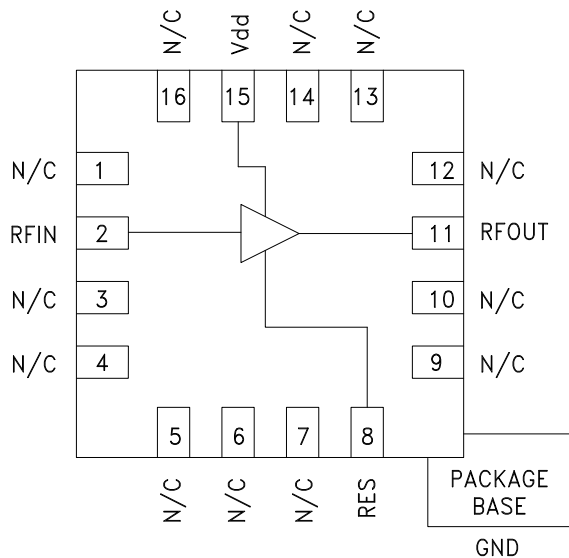
The HMC715LP3(E) is ideal for:

- Cellular/3G and LTE/WiMAX/4G
- BTS & Infrastructure
- Repeaters and Femtocells
- Public Safety Radio
- Access Points

Features

- Noise Figure: 0.9 dB
- Gain: 19 dB
- Output IP3: +33 dBm
- Single Supply: +3V to +5V
- 16 Lead 3x3mm QFN Package: 9 mm²

Functional Diagram



General Description

The HMC715LP3(E) is a GaAs PHEMT MMIC Low Noise Amplifier that is ideal for Cellular/3G and LTE/WiMAX/4G basestation front-end receivers operating between 2.1 and 2.9 GHz. The amplifier has been optimized to provide 0.9 dB noise figure, 19 dB gain and +33 dBm output IP3 from a single supply of +5V. Input and output return losses are excellent and the LNA requires minimal external matching and bias decoupling components. The HMC715LP3(E) can be biased with +3V to +5V and features an externally adjustable supply current which allows the designer to tailor the linearity performance of the LNA for each application.

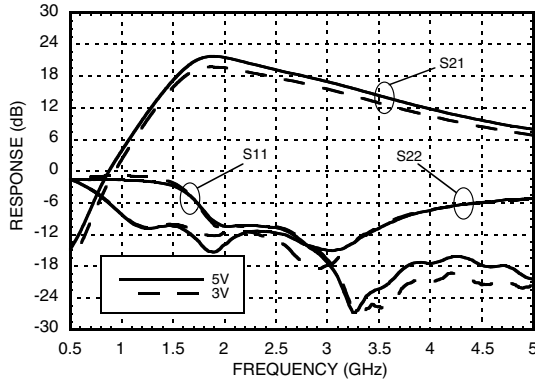
Electrical Specifications

$T_A = +25^\circ\text{C}$, $R_{bias} = 2k\text{ Ohms}$ for $V_{dd} = +5V$, $R_{bias} = 47k\text{ Ohms}$ for $V_{dd} = +3V$ [1]

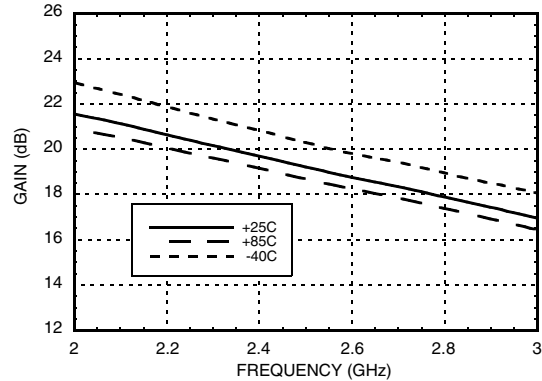
Parameter	Vdd = +3V			Vdd = +5V			Vdd = +3V			Vdd = +5V			Units
	Min.	Typ.	Max.	Min.	Typ.	Max.	Min.	Typ.	Max.	Min.	Typ.	Max.	
Frequency Range	2.1 - 2.9			2.3 - 2.7			2.1 - 2.9			2.3 - 2.7			MHz
Gain	14.5	18		15	18		15.5	19		16.5	19		dB
Gain Variation Over Temperature		0.01			0.01			0.01			0.01		dB/°C
Noise Figure		0.9	1.2		0.9	1.2		0.9	1.2		0.9	1.2	dB
Input Return Loss		11.5			11			11.5			11		dB
Output Return Loss		14			13.5			12.5			12		dB
Output Power for 1 dB Compression (P1dB)	10.5	14.5		12.5	15		15	19		16.5	19.5		dBm
Saturated Output Power (Psat)		16			16.5			20			20.5		dBm
Output Third Order Intercept (IP3)		28			28.5			33			33.5		dBm
Supply Current (Idd)		47	65		47	65		95	126		95	126	mA

[1] Rbias resistor sets current, see application circuit herein

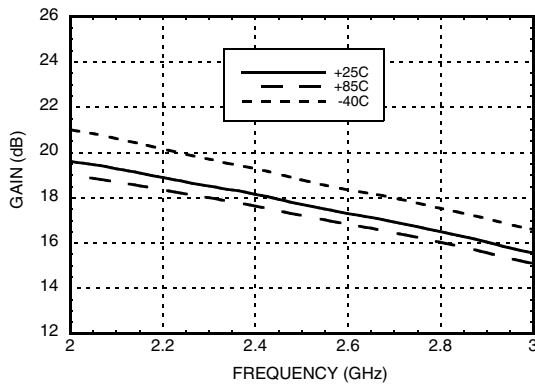
Broadband Gain & Return Loss [1] [2]



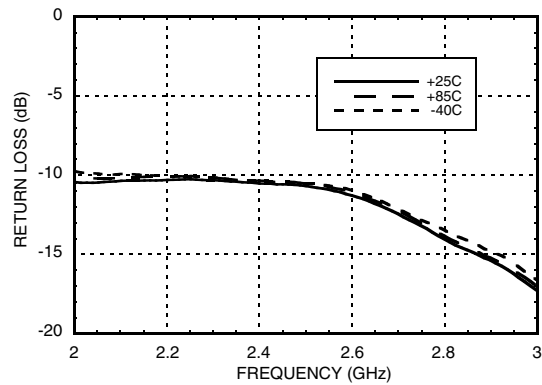
Gain vs. Temperature [1]



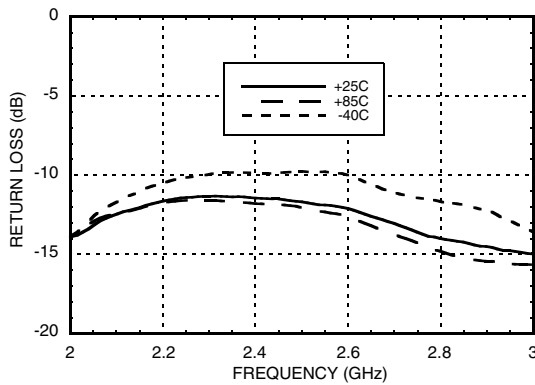
Gain vs. Temperature [2]



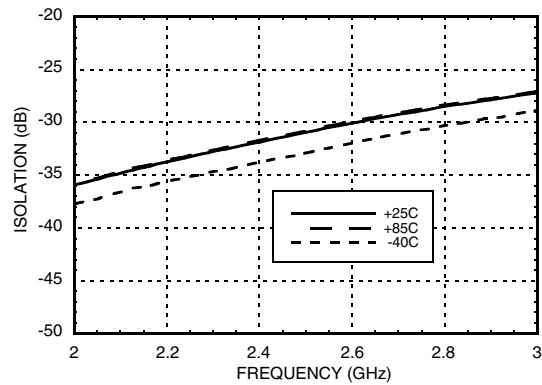
Input Return Loss vs. Temperature [1]



Output Return Loss vs. Temperature [1]

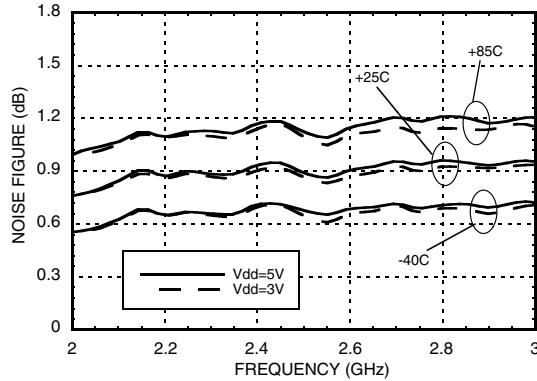


Reverse Isolation vs. Temperature [1]

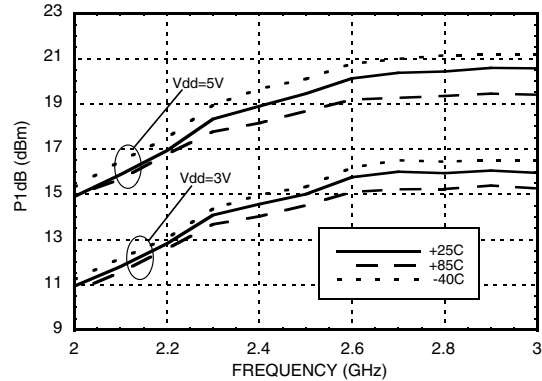


[1] Vdd = 5V, Rbias = 2kΩ [2] Vdd = 3V, Rbias = 47kΩ

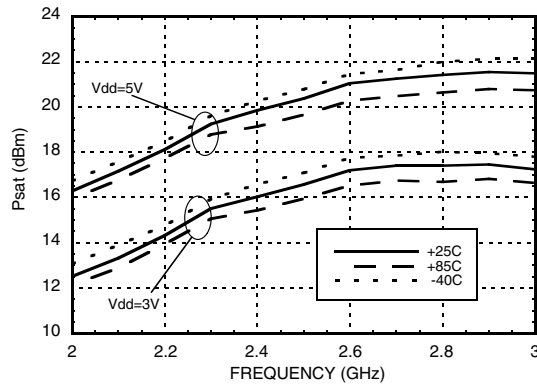
Noise Figure vs. Temperature [1] [2] [4]



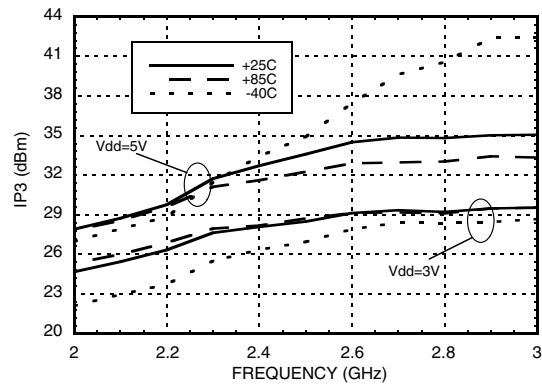
P1dB vs. Temperature [1] [2]



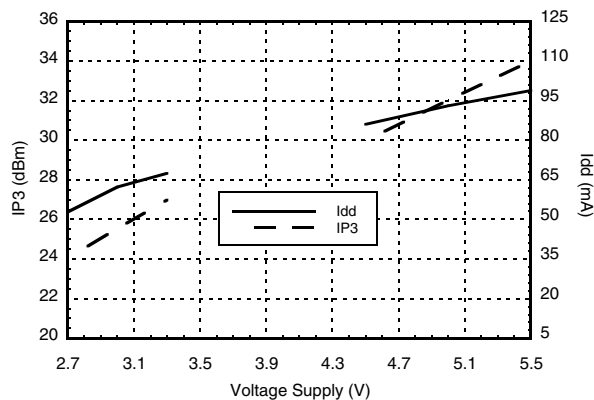
Psat vs. Temperature [1] [2]



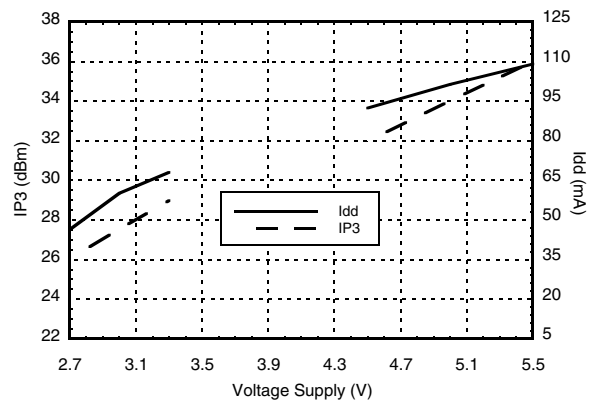
Output IP3 vs. Temperature [1] [2]



Output IP3 and Supply Current vs. Supply Voltage @ 2300 MHz [3]



Output IP3 and Supply Current vs. Supply Voltage @ 2700 MHz [3]

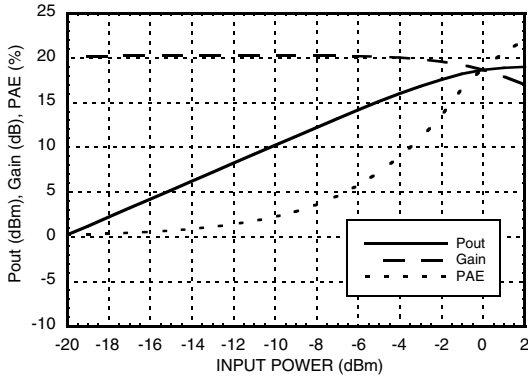


[1] V_{dd} = 5V, R_{bias} = 2kΩ [2] V_{dd} = 3V, R_{bias} = 47kΩ

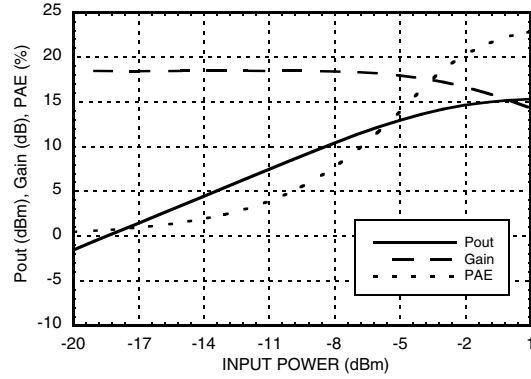
[3] R_{bias} = 2kΩ for V_{dd} = 5V, R_{bias} = 47kΩ for V_{dd} = 3V [4] Measurement reference plane shown on evaluation PCB drawing.



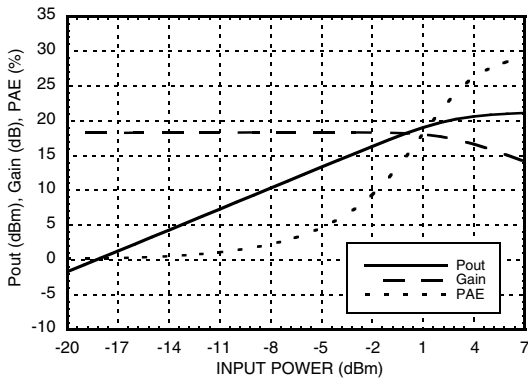
Power Compression @ 2300 MHz [1]



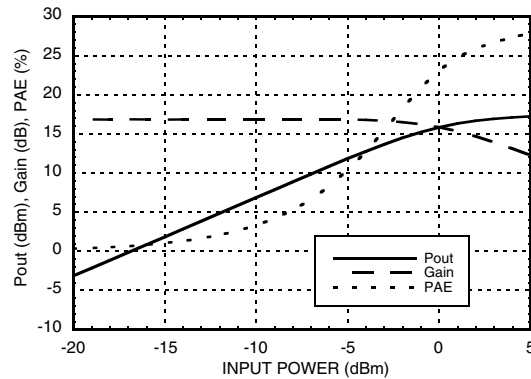
Power Compression @ 2300 MHz [2]



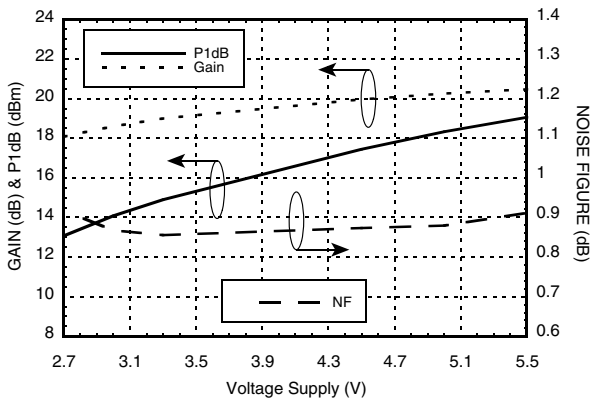
Power Compression @ 2700 MHz [1]



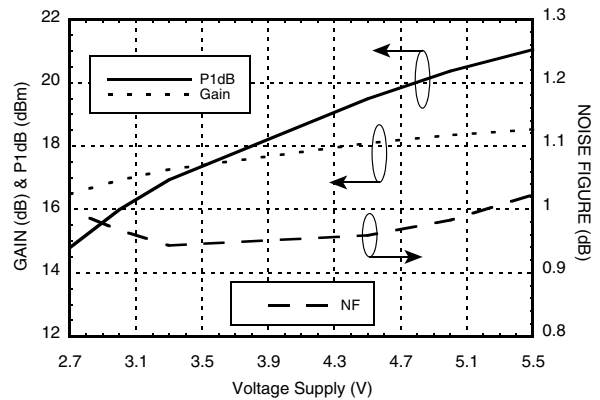
Power Compression @ 2700 MHz [2]



Gain, Power & Noise Figure vs. Supply Voltage @ 2300 MHz [3]

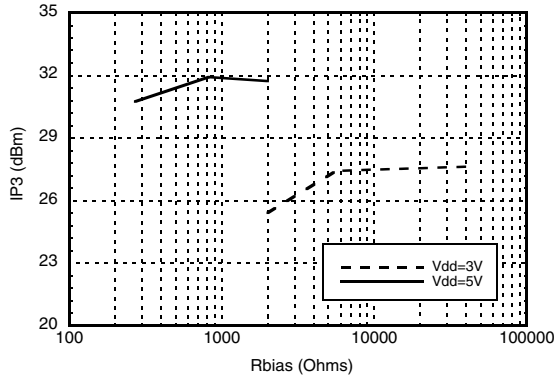


Gain, Power & Noise Figure vs. Supply Voltage @ 2700 MHz [3]

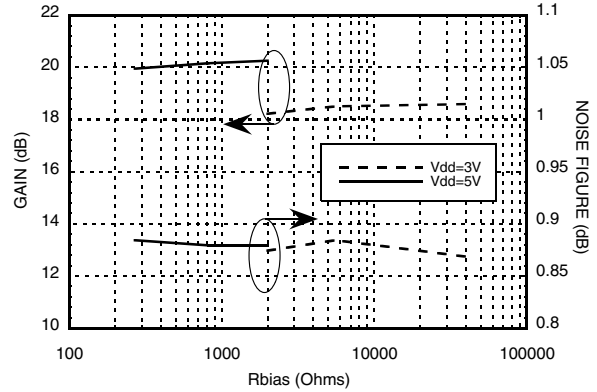


[1] Vdd = 5V, Rbias = 2kΩ [2] Vdd = 3V, Rbias = 47kΩ [3] Rbias = 2kΩ for Vdd = 5V, Rbias = 47kΩ for Vdd = 3V

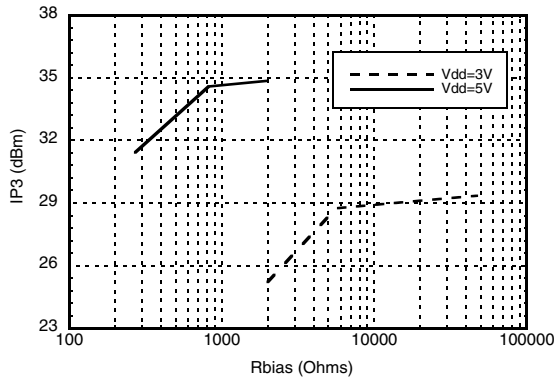
Output IP3 vs. Rbias @ 2300 MHz



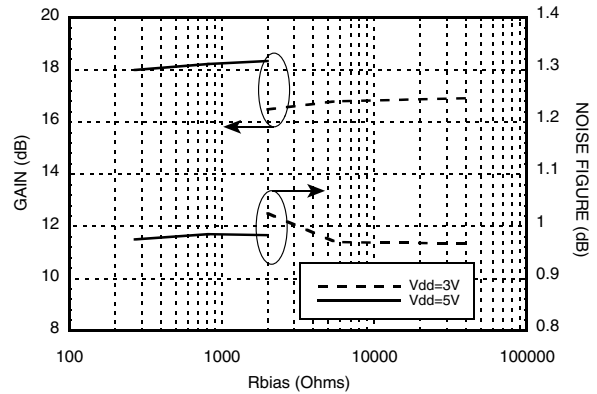
Gain, Noise Figure & Rbias @ 2300 MHz



Output IP3 vs. Rbias @ 2700 MHz



Gain, Noise Figure & Rbias @ 2700 MHz




**Absolute Bias Resistor
Range & Recommended Bias Resistor Values**

Vdd (V)	Rbias (Ohms)			Idd (mA)
	Min	Max	Recommended	
3V	1.8k [1]	Open Circuit	2K	28
			5.6K	40
			47K	47
5V	0	Open Circuit	270	61
			820	81
			2K	95

[1] With Vdd= 3V and Rbias < 1.8k Ohms may result in the part becoming conditionally stable which is not recommended.

Absolute Maximum Ratings

Drain Bias Voltage (Vdd)	+5.5V
RF Input Power (RFIN) (Vdd = +5 Vdc)	+10 dBm
Channel Temperature	150 °C
Continuous P _{diss} (T= 85 °C) (derate 11.1 mW/°C above 85 °C)	0.72 W
Thermal Resistance (channel to ground paddle)	90 °C/W
Storage Temperature	-65 to +150 °C
Operating Temperature	-40 to +85 °C
ESD Sensitivity (HBM)	Class 1A



**ELECTROSTATIC SENSITIVE DEVICE
OBSERVE HANDLING PRECAUTIONS**

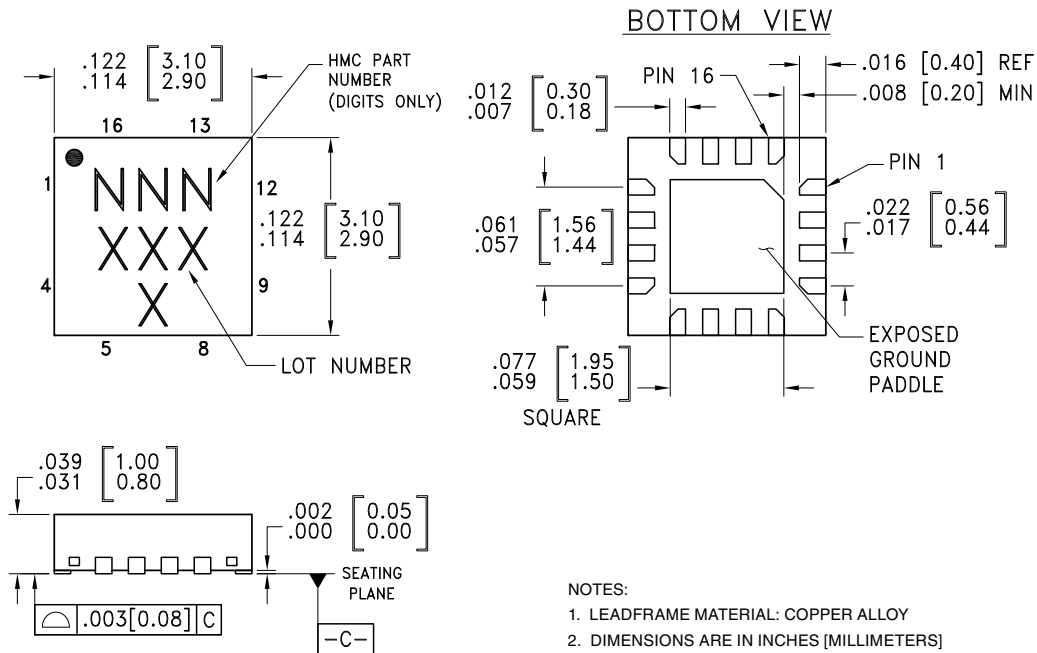
Typical Supply Current vs. Supply Voltage

(R_{bias} = 2k for Vdd = 5V, R_{bias} = 47k for Vdd = 3V)

Vdd (V)	Idd (mA)
2.7	35
3.0	47
3.3	57
4.5	80
5.0	95
5.5	110

Note: Amplifier will operate over full voltage ranges shown above.

Outline Drawing



NOTES:

1. LEADFRAME MATERIAL: COPPER ALLOY
2. DIMENSIONS ARE IN INCHES [MILLIMETERS]
3. LEAD SPACING TOLERANCE IS NON-CUMULATIVE
4. PAD BURR LENGTH SHALL BE 0.15mm MAXIMUM.
PAD BURR HEIGHT SHALL BE 0.05mm MAXIMUM.
5. PACKAGE WARP SHALL NOT EXCEED 0.05mm.
6. ALL GROUND LEADS AND GROUND PADDLE MUST BE SOLDERED TO PCB RF GROUND.
7. REFER TO HITTITE APPLICATION NOTE FOR SUGGESTED LAND PATTERN.

Package Information

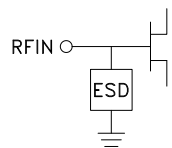
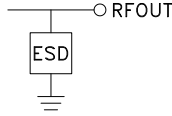
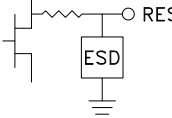
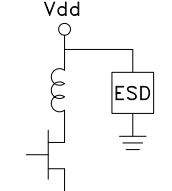
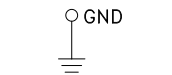
Part Number	Package Body Material	Lead Finish	MSL Rating	Package Marking ^[3]
HMC715LP3	Low Stress Injection Molded Plastic	Sn/Pb Solder	MSL1 ^[1]	715 XXXX
HMC715LP3E	RoHS-compliant Low Stress Injection Molded Plastic	100% matte Sn	MSL1 ^[2]	715 XXXX

[1] Max peak reflow temperature of 235 °C

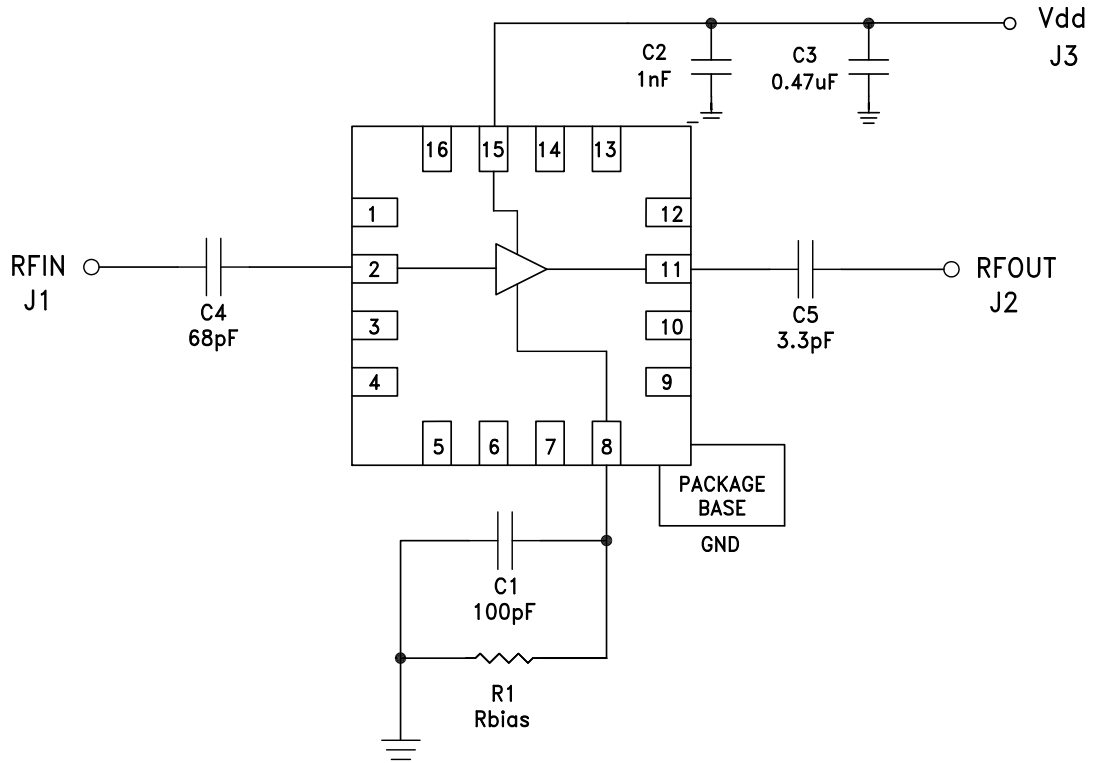
[2] Max peak reflow temperature of 260 °C

[3] 4-Digit lot number XXXX

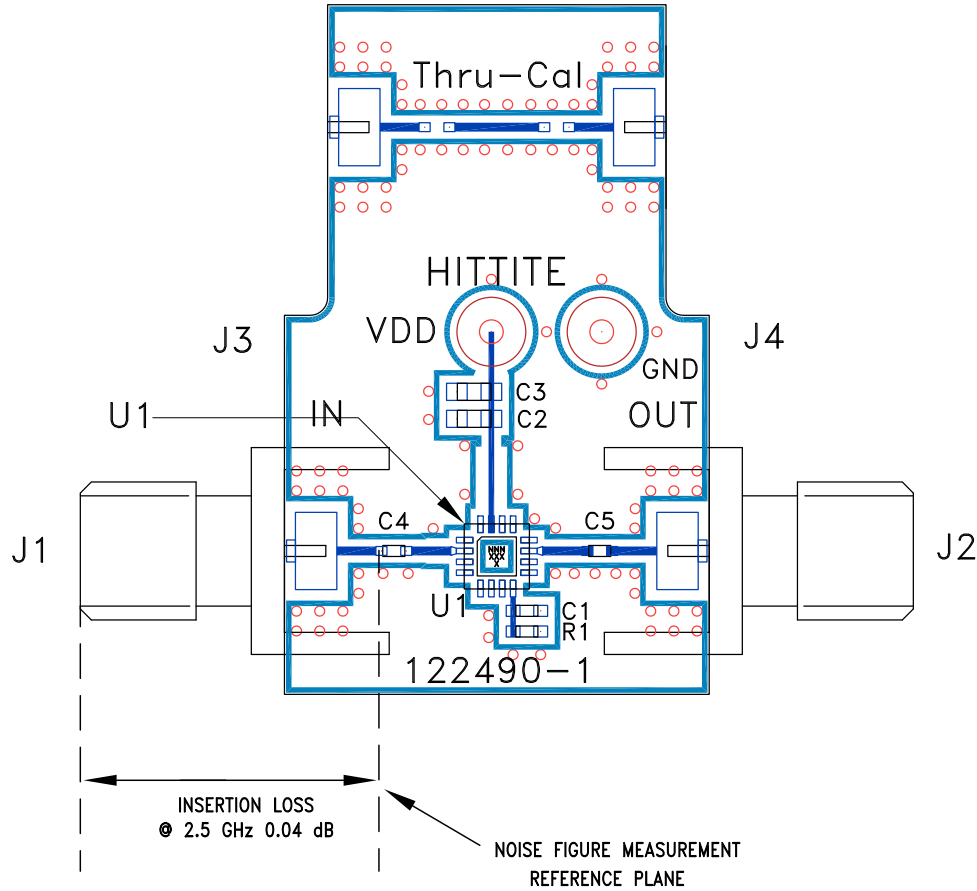

Pin Descriptions

Pin Number	Function	Description	Interface Schematic
1, 3 - 7, 9, 10, 12 - 14, 16	N/C	No connection required. These pins may be connected to RF/DC ground without affecting performance.	
2	RFIN	This pin is DC coupled. See application circuit for off chip component.	
11	RFOUT	This pin is DC coupled. See application circuit for off chip component.	
8	RES	This pin is used to set the DC current of the amplifier by selection of external bias resistor. See application circuit.	
15	Vdd	Power supply voltage. Bypass capacitors are required. See application circuit.	
	GND	Ground paddle must be connected to RF/DC ground.	

Application Circuit



Evaluation PCB



List of Materials for Evaluation PCB 122492 [1]

Item	Description
J1, J2	PCB Mount SMA RF Connector
J3, J4	DC Pin
C1	100pF Capacitor, 0402 Pkg.
C2	1000 pF Capacitor, 0603 Pkg.
C3	0.47µF Capacitor, 0603 Pkg.
C4	68pF Capacitor, 0402 Pkg.
C5	3.3pF Capacitor, 0402 Pkg.
R1	2kΩ Resistor, 0402 Pkg.
U1	HMC715LP3(E) Amplifier
PCB [2]	122490 Evaluation PCB

[1] Reference this number when ordering complete evaluation PCB

[2] Circuit Board Material: Rogers 4350. or Arlon 25R

The circuit board used in this application should use RF circuit design techniques. Signal lines should have 50 Ohm impedance while the package ground leads and exposed paddle should be connected directly to the ground plane similar to that shown. A sufficient number of via holes should be used to connect the top and bottom ground planes. The evaluation board should be mounted to an appropriate heat sink. The evaluation circuit board shown is available from Hittite upon request.

Coaxial Low Noise Amplifier

ZEL-1724LN+ ZEL-1724LN

50Ω 1700 to 2400 MHz

Features

- very low noise figure, 1.5 dB max.
- wideband, 1700 to 2400 MHz
- rugged, shielded case

Applications

- PCS/DCS
- UMTS
- communication systems



Connectors	Model	Price	Qty.
SMA	ZEL-1217LN(+)	\$274.95 ea.	(1-9)

Case Style: EEE132

+ RoHS compliant in accordance with EU Directive (2002/95/EC)

The +Suffix identifies RoHS Compliance. See our web site for RoHS Compliance methodologies and qualifications.

Electrical Specifications

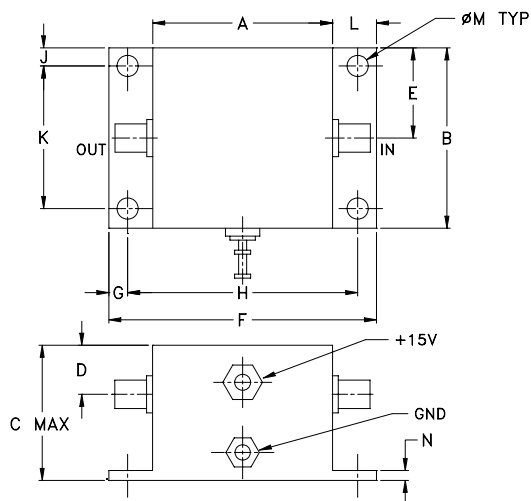
Parameter	Frequency (MHz)	Min.	Typ.	Max.	Units
Frequency Range		1700		2400	MHz
Noise Figure	1700-2400	—	—	1.5	dB
Gain	1700-2400	20	—	—	dB
Gain Flatness	1700-2400	—	—	±1.0	dB
Output Power at 1dB compression	1700-2400	—	+8	—	dBm
Output third order intercept point	1700-2400	—	+22	—	dBm
Input VSWR	1700-2400	—	—	2.5	:1
Output VSWR	1700-2400	—	—	2.5	:1
DC Supply Voltage		—	15	—	V
Supply Current		—	—	70	mA

Noise Figure specified at room temperature, increases to 2 dB typical at +85°C

Open load is not recommended, potentially can cause damage.

With no load derate max input power by 20 dB

Outline Drawing



Maximum Ratings

Parameter	Ratings
Operating Temperature	-54°C to 85°C
Storage Temperature	-55°C to 100°C
DC Voltage	17V
Input RF Power (no damage)	+13 dBm

Permanent damage may occur if any of these limits are exceeded.

Outline Dimensions (inch)

A	B	C	D	E	F	G	H	J	K	L	M	N	wt
.90	.90	.675	.245	.45	1.34	.09	1.152	.09	.712	.22	.106	.05	grams
22.86	22.86	17.15	6.22	11.43	34.04	2.29	29.26	2.29	18.08	5.59	2.69	1.27	50.0

Mini-Circuits®
ISO 9001 ISO 14001 AS 9100 CERTIFIED

P.O. Box 350166, Brooklyn, New York 11235-0003 (718) 934-4500 Fax (718) 332-4661 The Design Engineers Search Engine Provides ACTUAL Data Instantly at minicircuits.com

For detailed performance specs & shopping online see web site

IFIRF MICROWAVE COMPONENTS

Notes: 1. Performance and quality attributes and conditions not expressly stated in this specification sheet are intended to be excluded and do not form a part of this specification sheet. 2. Electrical specifications and performance data contained herein are based on Mini-Circuit's applicable established test performance criteria and measurement instructions. 3. The parts covered by this specification sheet are subject to Mini-Circuits standard limited warranty and terms and conditions (collectively, "Standard Terms"); Purchasers of this part are entitled to the rights and benefits contained therein. For a full statement of the Standard Terms and the exclusive rights and remedies thereunder, please visit Mini-Circuits' website at www.minicircuits.com/MCLStore/terms.jsp.

REV. A
M125917
ZEL-1724LN
100129
Page 1 of 2

Typical Performance Data/Curves

FREQUENCY (MHz)	GAIN (dB)			DIRECTIVITY (dB)			VSWR (:1)		NOISE FIGURE (dB)	POUT at 1 dB COMPR. (dBm)
	12V	15V	16V	12V	15V	16V	IN	OUT		
1700.00	22.23	22.96	23.14	12.70	12.80	12.70	1.61	1.64	1.28	11.46
1751.20	22.22	22.90	23.05	12.50	12.70	12.70	1.63	1.65	1.31	11.45
1821.90	22.16	22.78	22.91	12.60	12.70	13.00	1.66	1.65	1.40	11.64
1895.50	22.19	22.77	22.88	12.50	13.00	13.10	1.69	1.60	1.45	11.65
1969.20	22.29	22.79	22.90	12.30	12.40	13.00	1.68	1.55	1.47	11.79
2041.00	22.43	22.91	23.01	11.70	12.20	12.60	1.65	1.48	1.46	11.86
2130.80	22.78	23.21	23.29	10.80	11.90	12.20	1.55	1.38	1.39	12.00
2220.50	23.39	23.73	23.77	10.00	11.10	11.10	1.37	1.29	1.32	12.00
2310.30	23.58	23.96	24.02	9.30	9.90	10.20	1.23	1.38	1.31	11.58
2400.00	23.02	23.65	23.75	9.80	10.20	10.00	1.50	1.77	1.44	10.58

